Kinetics by thermal analysis

Reaction rates of processes involving solids with different specific surfaces
B.V Yerofeyev
Reactivity of solids 1961

Reaction kinetics by DTA
H.E. Kissinger
Anal Chem 1957

Analytical solution for Kissinger Equation
P. Roura, J. Farjas
J. Mater. Res. 2009

Data treatment in nonisothermal kinetics and diagnostic limits of phenomenological models
N. Koga, J. Malek, J. Sestak, H. Tanaka
Netsu Sukotei 1993

Forty years of Sestak-Berggren equation
P. Simon
Thermochim Acta 2011

Determination of activation energies by DTA
G.O. Piloyan, I.D. Ryabchikov, O.S. Novikova
Nature 1966

Diagnostic limits of phenomenological models of heterogeneous reactions and thermal analysis kinetics
J. Šesták, J. Málek
Solid State Ionics 1995

INTERNATIONAL SYMPOSIUM ON THERMAL ANALYSIS

13th and 14th April, 1965

CHEMISTRY DEPARTMENT
NORTHERN POLYTECHNIC
HOLLOWAY ROAD - LONDON - N.7

WEDNESDAY, 14th APRIL

MORNING SESSION

Chairman: Dr. R. C. MACKENZIE

9.30 a.m. Theatre A **"The Causes of Error in Thermogravimetry"**
Dr. M. HARMELIN (C.N.R.S., Paris)

10.45 a.m. Coffee

11.15 a.m. Theatre A **"Miscellaneous Thermal Methods"**
Prof. W. W. WENDLANDT (Texas Technological College)

12.30 p.m. Lunch

AFTERNOON SESSION

2.00 p.m. Theatre A Chairman: Dr. J. P. REDFERN
"Kinetic Studies by Thermogravimetry"
Dr. G. GUIOCHON (Ecole Polytechnique, Paris)

3.00 p.m. Tea

3.30 p.m. Theatre B **"Applications of Thermal Analysis to Inorganic Compounds II" (Papers B/5-9)**
Chairman: Dr. M. J. FRAZER

Theatre C **"Applications of Thermal Analysis to the Study of Organic Compounds (including Polymers)" (Papers C/5-9)**
Chairman: Mr. D. A. SMITH

Theatre D **"Techniques of Thermal Analysis II" (Papers D/5-9)**
Chairman: Dr. R. C. MACKENZIE

Close—5.30 p.m.

TUESDAY, 13th APRIL

MORNING SESSION

Chairman: Dr. J. P. REDFERN

9.20 a.m. Theatre A **Introduction by Dr. W. Gerrard**
(Head of the Chemistry Dept., Northern Polytechnic)

9.30 a.m. Theatre A **"Atmosphere Effects in Differential Thermal and Thermogravimetric Analysis"**
Prof. P. D. GARN (University of Akron, Ohio)

10.45 a.m. Coffee

11.15 a.m. Theatre A **"Derivatography"**
Prof. L. ERDEY (Technical University of Budapest)

12.30 p.m. Lunch

AFTERNOON SESSION

2.00 p.m. Theatre A **"General Aspects of Thermal Analysis" (Papers A/1-4)**
Chairman: Prof. P. D. GARN

3.30 p.m. Tea

4.00 p.m. Theatre B **"Applications of Thermal Analysis to Inorganic Compounds I" (Papers B/1-4)**
Chairman: Prof. W. W. WENDLANDT

Theatre C **"Applications of Thermal Analysis to Polymer Studies" (Papers C/1-4)**
Chairman: Mr. D. A. SMITH

Theatre D **"Techniques of Thermal Analysis I" (Papers D/1-4)**
Chairman: Dr. B. R. CURRELL

Close—5.30 p.m.

KEY LECTURES "A"

"General Aspects of Thermal Analysis"

Chairman: Professor P.D. Garn

Theatre A Tuesday: 2.00 - 3.30 p.m.

A1 "The Standardisation of Experimental Conditions in Thermal Analysis"
F. Paulik and J. Paulik (Technical University of Budapest)

A2 "Procedural Variables Influencing the Thermogravimetric Study of Polymer Decomposition"
D.A. Smith (National College of Rubber Technology, London)

A3 "The Use of Thermal Standards in Thermogravimetric Analysis"
C.J. Keattch (John Laing Research and Development Ltd., Boreham Wood)

A4 "The Error of Kinetic Data Obtained from Thermogravimetric Traces at a Rising Temperature"
J. Sestak (Institute of Solid State Physics, Czechoslovakia)

Reactivity of Solids, Proceedings of the 4th International Symposium (Amsterdam 1960): Amsterdam: Elsevier 1961 pp. 273-282

REACTION RATE OF PROCESSES INVOLVING SOLIDS WITH DIFFERENT SPECIFIC SURFACES

B. V. EROFEEV

Institute of Physical Organic Chemistry,
Academy of Sciences of the B.S.S.R., Minsk (U.S.S.R.)

The known equation

$$d\alpha/dt = k^1\alpha^{\frac{2}{3}}(1-\alpha)^{\frac{2}{3}} \quad (1)$$

is based on the proportionality between the reaction rate of chemical changes involving solids and the surface areas of an initial solid and a solid product. Starting from the topokinetic equation

$$\alpha = 1 - \exp(-kt^n) \quad (2)$$

which describes the progress of some reactions proceeding through the formation and growth of nuclei of the solid product, an approximate expression is obtained for the rate

$$d\alpha/dt = k^1\alpha^x(1-\alpha)^y \quad (3)$$

where values of x and y depend on the value of n in equation (2). The exponents $x = \frac{1}{2}, \frac{2}{3}, \frac{3}{4}\ldots$ and $y = 0.77, 0.70, 0.66\ldots$ correspond to whole-number values of n equal to 2, 3, 4 . . . . A comparison of (3) with data on the kinetics of polymorphic transformations of NH_4NO_3 confirms the existence of a relationship between n in (2) and x and y in (3). An investigation of the dependence of the rate of thermal decomposition of $KMnO_4$ and $(NH_4)_2Cr_2O_7$ on the surface area of the initial substances shows that the external surface of a solid substance plays different roles in different reactions. The initial decomposition rate (V_0) increases directly with the specific surface (S_0) of $KMnO_4$. The maximum decomposition rate (V_m) depends upon surface area slightly.

An analysis on the basis of equation (2) of possible changes in V_m when S_0 increases agrees generally with experiments.

Essentially different results were obtained during an investigation of the rate of thermal decomposition of ammonium dichromate samples with different specific surfaces. Rate-time curves for $(NH_4)_2Cr_2O_7$ samples with small surface have one maximum, as was observed by previous investigators. At 190° this maximum is reached in 60–70 minutes. When the specific surface increases a new rate maximum appears which at 190° is observed in 9–10 minutes. The larger the specific surface, the higher the first maximum rate. The value of the second maximum rate of decomposition decreases with an increase in the specific surface. Gas evolving at the time of the first maximum consists mainly of condensable gases such as NH_3 and N_2O, while gas evolving at the time of the second maximum contains a considerably smaller fraction of condensable gases. This would indicate that during decomposition of $(NH_4)_2Cr_2O_7$ two kinds of centres exist, for instance, surface centres and volume centres. When the specific surface increases, the reaction taking place as a result of the growth of surface centres acquires greater importance.

Although at the present time there are reliable methods of determining the surfaces of solid substances, the study of the reaction rate of processes involving solids depending on surface area has not received its due share of attention. Indirectly the role of surfaces in reactions proceeding through the formation and growth of nuclei of a solid product is assumed by the known equation

$$\frac{d\alpha}{dt} = k^1\alpha^{\frac{2}{3}}(1-\alpha)^{\frac{2}{3}} \quad (1)$$

References p. 280

However, the validity of this equation with regard to reactions involving solids is limited. This equation is valid for reactions in which kinetics are described by the topokinetic equation

$$\alpha = 1 - e^{-kt^n} \tag{2}$$

only on condition that $n = 3$. The expression for rate

$$\frac{d\alpha}{dt} = nk^{1/n}\left[-\ln(1-\alpha)^{1-1/n}\right](1-\alpha) \tag{3}$$

is derived from equation (2). The problem then is of finding optimal values for x and y in the equation

$$\frac{d\alpha}{dt} = k'\alpha^x(1-\alpha)^y \tag{4}$$

in order to replace (3) by an approximate expression having the form (4). The solution of this problem gives[1] $x = \frac{1}{2}, \frac{2}{3}, \frac{3}{4}, \frac{4}{5} \ldots 1$, and $y = 0.774, 0.700, 0.664, 0.642 \ldots 0.556$, corresponding to whole number values $n = 2, 3, 4, 5 \ldots \infty$.

Fig. 1 gives data on the transformation rate of NH_4NO_3 (III) $\rightarrow$ NH_4NO_3 (IV) for two of the experiments (for which $n = 2$). The data are plotted (a) in the coordinates $d\alpha/dt$ and $\alpha^{\frac{2}{3}}(1-\alpha)^{\frac{2}{3}}$, and (b) in the coordinates $d\alpha/dt$ and $\alpha^{\frac{1}{2}}(1-\alpha)^{0.774}$. The

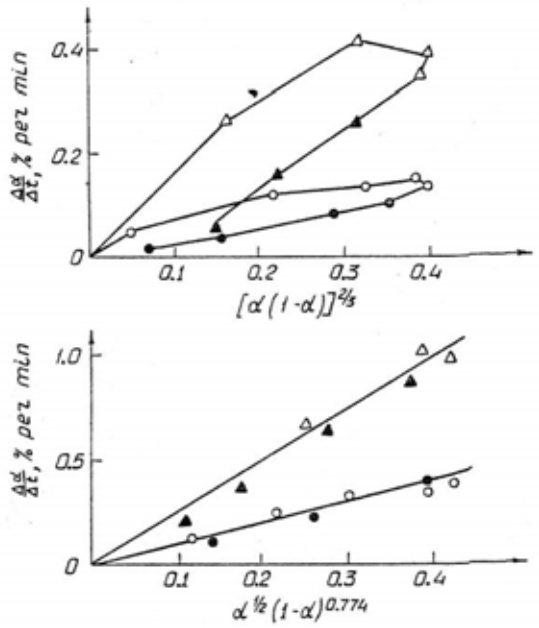

Fig. 1. Kinetics of transformation of NH_4NO_3 (III) $\rightarrow$ NH_4NO_3 (IV); $n = 2$; △ — experiment at 30.5°. ⊙ — experiment at 31.10°. Light points — value of rate before maximum; dark points — after maximum.

satisfactory application of equation (4) with values $x = \frac{1}{2}$ and $y = 0.774$ agrees with the value $n = 2$, while the same equation (4) with values $x = y = \frac{2}{3}$ does not describe satisfactorily the experimental data.

Fig. 2 gives data from an experiment on the thermal decomposition of potassium

References p. 280

permanganate. When the graph with coordinates ln [— ln (1 — α)] and ln t (α > 0.1) is plotted for this experiment it gives $n = 5$. In accordance with the above, the experimental data give a straight line in coordinates dα/dt and $\alpha^{0.8}(1-\alpha)^{0.642}$ (α > 0.03) but do not give a straight line in coordinates dα/dt and $\alpha^{\frac{2}{3}}(1-\alpha)^{\frac{2}{3}}$.

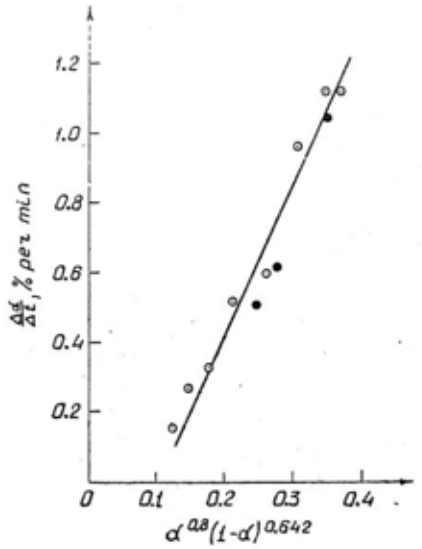

Fig. 2. Kinetics of thermal decomposition of $KMnO_4$, 218° C; $n = 5$.

Thus the real relationships between the reaction rate and surface area of the original solid substance and that of the solid product are more complex than would appear from equation (1).

It is interesting to note that with an increase in "n" the rate becomes proportional rather to the quantity of the solid product than to its surface area. Insufficiency of equation (1) to describe the reaction kinetics of the processes involving solids is connected with at least two circumstances: (1) Not the whole surface but only a part of it which changes during the course of the reaction is the place of reactions; (2) the size of solid particles is varied and for this reason the proportionality between S_1 and $\alpha^{\frac{2}{3}}$ or S_2 and $(1-\alpha)^{\frac{2}{3}}$ assumed in the derivation of the equation (1) does not hold.

The direct experimental investigation of the dependence of rate on surface area would require separate determinations: (1) of the surface of the original substance and (2) of the solid product in various stages of the reaction, while the existing methods permit the determination only of the total surface of both substances present. Moreover, it would be necessary to use an independent method for the determination of the surface of contact between two solid substances. Apparently considerable time will pass before the solution of this problem is reached.

In connection with these difficulties it seems consistent to investigate a less fundamental but simpler problem, namely the question of the dependence of the reaction rate on the initial surface of the original solid substance. Such investigations were carried out by V. A. Protashchik on $KMnO_4$ and by N. G. Peryshkina on $(NH_4)_2Cr_2O_7$ in our laboratory.

Samples with different surfaces were obtained by means of grinding followed by passing through a set of sieves. In most of the cases the surface was determined by the method of sucking air through a layer of the solid in conditions of Knudsen's

References p. 280

regime of pressure. Deryaguine's apparatus was used for this purpose[2]. The control measurements of surfaces of some samples of $KMnO_4$ by the BET method gave similar results (Table I), though the BET method was less accurate for the determination of low surface areas ($< 1\ m^2$) than Deryaguine's method.

The investigation of the decomposition rate was made by determining the pressure of gaseous products with an initial vacuum of $\sim 10^{-6}$ mm.

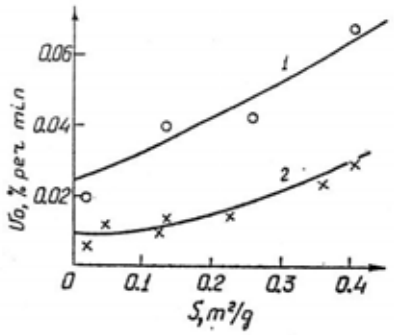

Fig. 3. Initial rate of decomposition of $KMnO_4$ depending on specific surface. (1) Kinetics of decomposition of $KMnO_4$ 2 months after preparation; (2) preparation aged for 14 months; (218°).

The initial decomposition rate was extrapolated from the first experimental points. Fig. 3 gives the dependence of the initial decomposition rate, determined in this way, on the surface area of the samples of $KMnO_4$ aged for 2 and 14 months after recrystallization.

TABLE I

Sample of $KMnO_4$	I-2	I-3
Surface area by the Deryaguine method m^2/g	0.14	0.23
The same by the BET method m^2/g	$\sim$ 0.1	$\sim$ 0.2

Fig. 3 shows that the initial rate increases with an increase in surface area. The trend of experimental points shows that the rate increment increases proportionally not to the first but to a higher power of surface area. This would indicate that the initial reaction centres are mainly situated on the edges or the polyhedral angles of crystals. Both curves shown in Fig. 3 intersect the positive branch of the ordinate axis. The length of cut-off sections represent that part of the initial rate which does not depend on surface area and is dependent on the process starting in the interior of the crystals. The largest part of the initial rate of samples with low surface area is dependent on the volume process.

The existence of the decomposition process within the crystals explains the well-known splitting of crystals of $KMnO_4$. A reduction of initial rate is observed following the aging of the $KMnO_4$ preparations. Fig. 3 shows that a reduction of rate occurs both for the surface and for the volume decomposition process. A reduction of volume rate of the process can apparently be explained only as a result of a decrease in the number of crystal lattice defects during aging. It is possible that the decrease in the surface process rate occurs as a result not only of the decrease in the number of lattice defects but also of the formation on the surface layer of substances which inhibit the formation of initial decomposition centres.

References p. 280

In order to verify this assumption, experiments were undertaken in the decomposition of old $KMnO_4$ preparations before and after washing them with water. Washing was done on a funnel with a glass filter, using a small quantity of water After washing the initial decomposition rate increases (Table II).

TABLE II

Surface before washing, m^2	0.14
Initial rate before washing	0.007
Initial rate after washing	0.030

Samples of $KMnO_4$ on which the experiments were made had been prepared by passing a non-recrystallized commercial preparation of $KMnO_4$ through a sieve. The data in Table II may naturally be complicated by the fact that washing may alter their surface area.

The effect of surface area upon the maximum decomposition rate of $KMnO_4$ is considerably less, as in apparent from Table III which gives data for the same experiments from which the relationship between initial rate and surface area were obtained in Fig. 3.

TABLE III

	$KMnO_4$ after 2nd month of aging				*$KMnO_4$ after 14th month of aging*						
S, m^2/g	0.02	0.14	0.23	0.41	0.02	0.05	0.13	0.14	0.23	0.36	0.41
V_m, % min^{-1}	1.18	0.63	0.68	0.70	1.15	1.10	1.10	1.15	1.18	1.10	1.00

As Table III shows, the maximum rate is much less dependent upon surface area than initial rate. For fresher preparations the maximum rate decreases to one-half with an increase in surface area from 0.02 to 0.14 m^2/g. The increase of the surface area over 0.14 m^2/g as a fact does not influence the maximum rate. For older samples the rate is about constant notwithstanding the surface increase. The slight dependence of maximum rate on surface area can be understood on the basis of the topokinetic equation (2), which gives an expression for maximum rate:

$$V_m = K^{1/n} n^{1/n} (n-1)^{(1-1/n)} e^{(-1+1/n)}.$$

K is proportional to the rate of formation of initial centres of reaction which in its turn depends on surface area. Thus with $n = 5$, $K = (2\omega/5!)\,\kappa_1\kappa_2 v_0 u^3$ where v_0 is the number of potential centres on which nuclei of solid products may be formed[3]. If these centres are situated on the surface, then v_0 and therefore K is proportional to the surface. However, since K is raised to the $1/n$th power, the dependence of V_m on surface area is slight. The experiment shows that the change of surface area also affects the value of n. This follows from Fig. 4, in which data for aged samples are plotted in coordinates $\ln[-\ln(1-\alpha)]$ and $\ln t$.

For the majority of preparations the experimental points lie on two straight lines which intersect each other. The point of intersection corresponds to a degree of

References p. 280

transformation of from 10% to 30%. Thus most of the transformation of all 70% or 90% is described by a single straight line, the tangent of slope of which decreases from 5 to 3 with an increase in surface area.

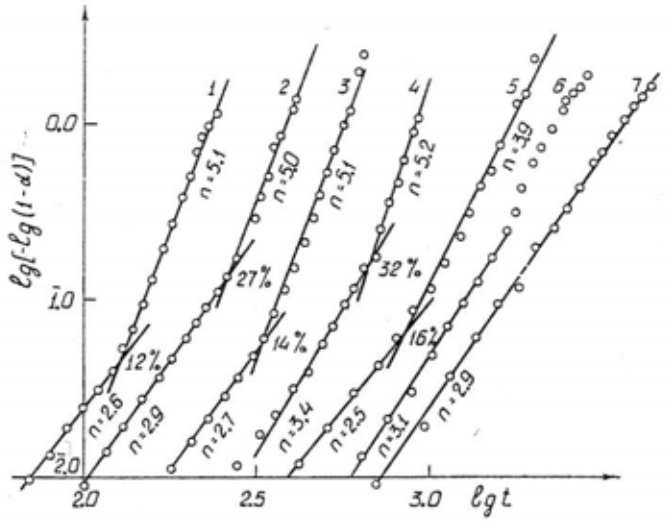

Fig. 4. Kinetics of decomposition of aged preparations of $KMnO_4$ with different specific surface value (218°). (1) 0.023 m^2/g; (2) 0.047 m^2/g; (3) 0.125 m^2/g; (4) 0.137 m^2/g; (5) 0.230 m^2/g; (6) 0.359 m^2/g; (7) 0.406 m^2/g. Origin of coordinates for lines 2, 3, 4, 5, 6 and 7 displaced to the right by 0.2; 0.4; 0.6; 1.0; 1.10 and 1.35 scale units.

The straight lines passing through the points corresponding to the first 10%–30% of decomposition have tangents of slope 2.5–3. For samples with a smaller surface area the decomposition is described by a straight line of value $n = 5$. As shown above, most of the initial rate for these samples is due to the volume process. Consequently the value $n = 5$ should be ascribed to the volume process. The point initial decomposition centres formed as a result of two consecutive processes, as for instance

$$2MnO_4' \rightarrow MnO_4''' + MnO_2^+ + O_2;\ MnO_4' + MnO_2^+ \rightarrow Mn^{+++} + MnO_4''' + O_2$$

correspond to this value.

The formation of the ion MnO_4''' should be given preference to the formation of MnO_4'' since the ion MnO_4''' is only weak by colour[4]. The absence of deep colour in the solutions of the decomposition products of $KMnO_4$ agrees with this.

The greater the surface area, the greater the degree of decomposition which is described by the straight line with a tangent of slope 3. For the preparation with the largest investigated surface of 0.4 m^2/g the total decomposition is described by a straight line with a slope of 3. The major part of initial rate in this experiment is also conditioned by the surface process.

An investigation of the thermal decomposition of ammonium dichromate with different specific surface area reveals the existence of two processes distinct in time, which have not been mentioned by the previous investigators of this reaction. In contradistinction to that of $KMnO_4$, the extrapolation of first points gives the value of zero for the initial rate within the limits of accuracy of measurement. For whole crystals of $(NH_4)_2Cr_2O_7$ and for samples with surface of less than 0.1 m^2, pressure-time curves have the same form as that obtained by other authors[5,6]. However, if we

References p. 280

consider rate-time curves (Fig. 5), as for samples with a surface area of 0.05 and above, we note two rate maxima: the first taking place at about the 9th minute and the second at 60–70 minutes. For preparations with a large surface area, the first maximum is the main one, and the second maximum nearly disappears. It was possible to calculate the quantity of gases evolving during the first and second processes. On Fig. 6 the quantity of gases evolving at the end of the first maximum is

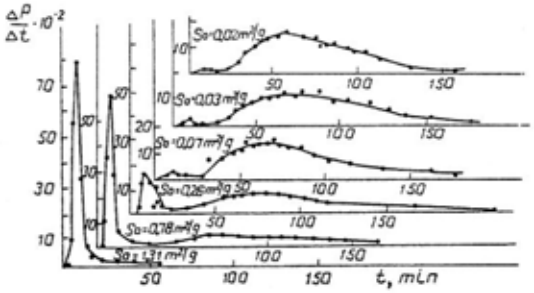

Fig. 5. Kinetics of decomposition of preparations of $(NH_4)_2Cr_2O_7$ with different specific surface, 190°.

deposited as a function of surface area. Apparently a direct proportionality exists between quantity of gases and surface area when the surface areas are small. This proves the surface character of the first process. The depth of the surface layer affected by this process can be estimated from the formula $h = B/mN$, where h is the depth expressed as the number of layers of elementary cells, B the number of gas molecules evolving from one square meter of surface, m is the number of molecules of gaseous products evolving from one molecule of dichromate and N the number of molecules of dichromate situated per one square meter of surface. In this case it would seem

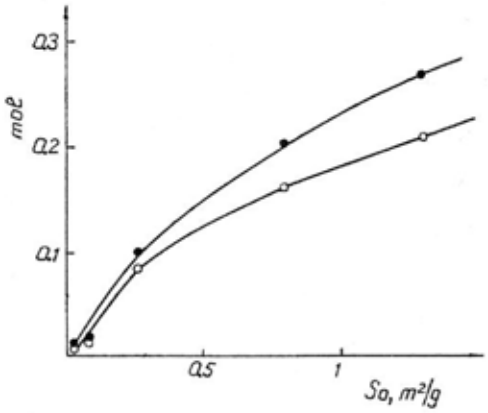

Fig. 6. Total quantity of gas (upper curve) and quantity of condensed gases (lower curve) evolved at first maximum of $(NH_4)_2Cr_2O_7$ decomposition as a function of specific surface.

reasonable to consider the dichromate molecules located within the surface crystal unit cells as surface molecules. A calculation of this kind gives approximately 4000 layers of unit cells which correspond to $5 \cdot 10^{-3}$ mm. With the dimensions of dichromate particles approaching this value, the largest quantity of gases should evolve during the first or the surface process. This agrees with the results of the experiment.

Experiments with freezing out condensing gases show that it is almost exclusively condensing gases which evolve in the first or the surface process. By the end of the

References p. 280

first maximum the quantity of not condensing gases does not exceed 5–6 %. However, at the later stages of reaction the proportion of condensing gases for samples with different surface area proves to be identical.

The quantity of gas evolving during the second process appears to be decreasing with an increase in surface area. Therefore this process should be considered as starting within the volume of solid particles. Thus the investigation of the kinetics of thermal decomposition of samples of potassium permanganate and ammonium dichromate with a different specific surface in both cases revealed the presence of two processes: (a) one starting on the surface and extending to the interior of the solid particles, and (b) another starting inside the solid particles.

REFERENCES

1. B. V. Erofeev and N. I. Mitskevich, *Collected Scientific Papers (Trudy) of Institute of Chemistry of the Academy of Scienes of the BSSR.* No. 5 (1956) 3.
2. B. V. Deryagin, N. N. Zakhavaeva, M. V. Talaev and V. V. Filippovskiĭ, *Determination of Specific Surface of Powdered Substances after Resisting Filtration of Rarified Air*, Academy of Sciences of the USSR, Moscow (1957).
3. B. V. Erofeev, *Collected Scientific Papers (Trudy) of Institute of Chemistry of the Academy of Sciences of the BSSR*, No. 5 (1956) 13.
4. E. Lux, *Z. Naturforsch.*, 1 (1946) 281.
5. K. Eischbeck and H. Spingler, *Z. anorg. u. allgem. Chem.*, 241 (1939) 209.
6. J. Simpson, D. Taylor and D. M. W. Anderson, *J. Chem. Soc.*, (1958) 2378.

DISCUSSION

K. K. Schiller, Eastleake, Leics. (Great Britain): I should like to mention some work which we have done and which deals also with a process obeying the $^2/_3$ power law mentioned by Prof. Erofeev. We have been working with the rehydration and setting of calcium sulphate hemihydrate which is usually allowed to take place in the form of dense slurries. Whilst this hydration process is known to take place through the solution this case is rather special insofar as the surface of the dissolving phase are bound to be very close to those of the new phase, although the nearest dissolving surface need not belong to the grain of the old phase on which the new crystal under consideration grows.

The hydration process is described by the chemical equation

$$CaSO_4 \cdot \tfrac{1}{2}\, H_2O + \frac{3}{2}\, H_2O = CaSO_4 \cdot 2\, H_2O\,.$$

As put down the equation shows the hydration of the plaster in which calcium sulphate *hemi*hydrate turns in calcium sulphate *di*hydrate and solidifies. The hemihydrate is a metastable phase in the calcium sulphate–water system and is obtained by calcining the mineral gypsum, a process described by reading the above chemical equation backwards. This calcination takes place at elevated temperatures as a transformation in the solid as described in the lecture by Prof. Ubbelohde.

The transformation of the hemihydrate into dihydrate goes through the solution. Hemihydrate which is more soluble than the dihydrate goes into solution and renders the solution supersaturated with respect to the dihydrate; this therefore precipitates and the exhausted solution is replenished by the dissolution of more hemihydrate and so on until all the hemihydrate is transformed into dihydrate

The hydration process is strongly exothermal and it can be shown that except certain extreme conditions the temperature rise under adiabatic conditions is a measure of the quantity of the new phase formed. When the temperature rise in a hydrating plaster slurry is plotted against time a sigmoid curve is obtained.

In our Laboratories in Eastleake we have developed a theory which quantitatively describes this process.

There are many reasons to assume that the nuclei on which the new phase grows are provided by surface irregularities or dislocations breaking through the surface of the hemihydrate.

On this basis and taking into account the special circumstances prevailing in a chemically unstable slurry the theory was developed and leads to the following experiment for the time required for 100 % of the stable phase to form

$$t = \frac{\rho}{\Delta \bar{c}} \left[\frac{\sqrt[3]{2}}{4\pi} \frac{V_0}{N^{2/3}} \frac{1}{D} \omega + \sqrt[3]{\frac{3}{4\pi}} \frac{1}{\gamma} \sqrt[3]{\frac{V_0}{N}} \sqrt[3]{\omega} + \sqrt[3]{\frac{3}{4t}} \frac{1}{\delta} \sqrt[3]{\frac{V_0}{N}} (1 - \sqrt[3]{1} - \omega) \right] \quad \text{(A)}$$

Diffusion term Growth term Dissolution term

where:

ϱ = density of dihydrate,
$\Delta \bar{c}$ = difference of solubilities of hemi- and dihydrate,
V_0 = volume of hemihydrate in 1 cm³ of slurry at the beginning
N = number of particles per cm³ of slurry,
D = average diffusion coefficient of anion and cation,
ω = percentage of new phase formed,
γ = mass deposited on a growing dihydrate crystal per unit time, unit area and unit absolute super-saturation,
δ = mass removed from a dissolving hemihydrate crystal per unit time, unit area and unit absolute under-saturation,
t = time elapsed since mixing the plaster and water to form the slurry.

On estimating orders of magnitude it can be shown that the first term, *i.e.* the diffusion term, can usually be neglected compared with the others. Theoretically, however, the diffusion process had to be taken into account as otherwise the fundamental equations would have had one unknown too many.

In the early stages when the percentage of stable phase, ω is still very small, only the middle term remains and $\omega \sim t^3$. This is a consequence of linear growth in all three directions.

As explained above ω will be proportional to the temperature rise in a thermal hydration test. According to the above formula a non-linear temperature scale can be designed which under certain circumstances should straighten the sigmoid hydration curve into an almost straight line. This has been found to be the case for near plasters, *i.e.* those which contain no chemical additions accelerating or retarding the process. The detailed features of the curve in cases where it deviates noticeably from a straight line promise to give indications of the mechanism of acceleration or retardation.

It can be shown that the above equation leads also to

$$\frac{d\omega}{dt} \sim \omega^{2/3} (1 - \omega)^{2/3} \quad \text{(B)}$$

if some simplifying assumptions are introduced.

A point which the writer has not seen mentioned before may also be made here. If we replace the index $^2/_3$ in eq. (B) by n it is seen that the time required to obtain a fraction ω of the new phase is given by

$$t = \int_0^t dt \sim \int_0^\omega \frac{d\omega}{\omega^n (1 - \omega)^n} \quad \text{(C)}$$

For small ω this is approximately

$$t \sim \int_0^\omega \frac{d\omega}{\omega^n} \quad \text{(D)}$$

This integral will duly converge if n is smaller than 1. Thus processes which react at a rate proportional to the product of the masses of the two phases present cannot start unless the lower limit of integral (D) is greater than 0, *i.e.* at least a trace of the new phase is present to sed the growth. For $n < 1$, for instance $n = {}^2/_3$, no such seeding is required.

Author's reply: Concerning the comments by Dr. Schiller on the equation (4), $\frac{d\alpha}{dt} = k\alpha^x (1 - \alpha)^y$, of my paper, I would like to note that this equation is derived by approximating the more precise expression (3) and is not very suitable for judgment about the very initial stage of reaction.

P. W. M. Jacobs, London (Great Britain): I should like to ask Prof. Erofeev what is his interpretation of a value of $n = 5$. In a solid–state decomposition, $n = 5$ implies that the number of nuclei increases as the square of the time, assuming growth is three-dimensional. I should also

like to ask how the decomposition rates of $(NH_4)_2Cr_2O_7$ were measured. Using an accumulatory technique, we find the $\alpha(t)$ curves are not fitted by the Erofeev equation (2) in your paper, but only by the unimolecular decay law which corresponds to the limiting case of $n = 1$. Is it possible that the reaction is retarded by the water formed? Certainly the final pressure is attained very slowly in this reaction.

A. ENGLANDER, Saclay (France): I am taking the opportunity to ask Prof. Erofeev if he can precise the physical meaning of the exponent or of his equation no. 2 when this is larger than 4.

Author's reply: In reply to Dr. Jacobs' and Dr. Englander's questions, the numerical value of $n \geqslant 5$ implies that the process of the formation of nuclei consists of two or more consecutive elementary stages, in which case the number of nuclei increases as the square or a higher power of the time.

As to the decomposition of $(NH_4)_2Cr_2O_7$ two rate maxima observed during the reaction imply that the nuclei form with different rates: (1) on the surface and (2) in the volume of solid particles and it makes the process of decomposition difficult to be described by the equation $\alpha = 1 - \exp(-kt^n)$ with the only value of "n". The unimolecular equation could not be applied to the initial part of the decomposition curve where the rate maximum is observed, but only to the final one. A study of the evolving rate of each gas component separately and of the influence of each one on the decomposition rate would be of value.

Groennings, S., ANAL. CHEM. **28**, 303 (1956).
(5) Heilbron, I. M., Kamm, E. D., Owens, W. M., *J. Chem. Soc.* **1926**, 1631.
(6) Isler, O., Rüegg, R., Chopard-dit-Jean, L., Bernhard, K., *Helv. Chim. Acta* **39**, 897 (1956).
(7) Karrer, P., Helfenstein, A., *Ibid.*, **14**, 78 (1931).
(8) Sax, K. J., Stross, F. H., *J. Org. Chem.* **22**, 1251 (1957).
(9) Schmitt, J., *Ann.* **547**, 115 (1941).
(10) Trippett, S., *Chem. & Ind. (London)* **1956**, 80.
(11) Tsujimoto, M., *Ind. Eng. Chem.* **8**, 889 (1916).
(12) Tunnicliff, D. D., Stone, H., ANAL. CHEM. **27**, 73 (1955).

RECEIVED for review January 15, 1957. Accepted July 8, 1957.

Reaction Kinetics in Differential Thermal Analysis

HOMER E. KISSINGER

National Bureau of Standards, Washington, D. C.

▶ **The effects of the kinetics of reactions of the type solid → solid + gas on the corresponding differential thermal analysis pattern are explored. Curves of reaction rate vs. temperature for constant heating rates constructed by analytical methods are used to demonstrate the effect of varying order of reaction. The information so obtained is used to analyze the differential thermal patterns of magnesite, calcite, brucite, kaolinite, and halloysite. The results of the differential thermal study agree with results obtained isothermally except in some specific cases.**

WHEN a reaction occurs in differential thermal analysis (DTA), the change in heat content and in the thermal properties of the sample is indicated by a deflection, or peak. If the reaction proceeds at a rate varying with temperature—i.e., possesses an activation energy—the position of the peak varies with the heating rate if other experimental conditions are maintained fixed. In a previous paper (*10*), it was demonstrated that this variation in peak temperature could be used to determine the energy of activation for first order reactions. The present paper extends the method to reactions of any order, and proposes a method for determining the order of reaction from the shape of the differential thermal analysis peak.

DIFFERENTIAL TEMPERATURE AND REACTION RATE

In previous work it was assumed that the temperature of maximum deflection in differential thermal analysis is also the temperature at which the reaction rate is a maximum. Because the proposed method for determining kinetic constants depends on the accuracy of this assumption, a more detailed discussion of its validity is given.

The temperature distribution in the differential thermal analysis specimen holders obeys the general heat flow equation (*11*).

$$\frac{\partial T}{\partial t} = \frac{k}{\rho c}\nabla^2 T + \frac{1}{\rho c}\frac{dq}{dt} \qquad (1)$$

where T is the temperature, t the time, k the thermal conductivity, ρ the density, c the specific heat, and dq/dt the rate of heat generation due to a chemical reaction per unit volume of sample. No heat effects occur in the reference sample, so the temperature distribution in the reference is given by:

$$\frac{\partial T}{\partial t} = \frac{k}{\rho c}\nabla^2 T \qquad (2)$$

If the sample is assumed to be a cylinder of radius a and of infinite length, with the temperature of the outside given by $T = T_0 + \phi t$, where ϕ is a constant rate of temperature rise and T_0 the initial temperature, the temperature at T_r at the center of the reference sample is, by integration of Equation 2 with proper limits,

$$T_r = T_0 + \phi t - \frac{\phi \rho c a^2}{4k} \qquad (3)$$

In Equation 1, the rate of heat generation is a function of temperature in the active sample. The equation then is a nonlinear partial differential equation, and cannot be solved by known analytical methods. We assume that, if the same boundary condition holds—i.e., that the temperature of the outside of the holder rises at a linear rate—the solution expressing the temperature at the center of the sample will be of the form:

$$T_s = T_0 + \phi t - f\left(\frac{dq}{dt}\right) \qquad (4)$$

where $f\left(\frac{dq}{dt}\right)$ is a function of the reaction rate which also includes any secondary effects of the reaction, such as changes in volume, density, or thermal properties.

The differential temperature is the difference in temperature of the centers of the two samples. The differential temperature, θ, is then given by

$$\theta = f\left(\frac{dq}{dt}\right)_{\text{sample}} - \left(\frac{\phi \rho c a^2}{4k}\right)_{\text{reference}} \qquad (5)$$

and

$$\frac{d\theta}{dt} = f'\left(\frac{dq}{dt}\right)\frac{d^2q}{dt^2} \qquad (6)$$

When θ is a maximum, $d\theta/dt$ is zero. From Equation 6 it is seen that when d^2q/dt^2, the derivative of the rate of heat absorption, is zero, $d\theta/dt$ is also zero. Since the rate of heat absorption is proportional to the rate of reaction, Equation 6 states that the peak differential deflection occurs when the reaction rate is a maximum. This is true only when the heating rate of the reference is constant, as otherwise Equation 6 would contain a derivative of ϕ.

A solution of the form of Equation 3 can be obtained for a sample of any shape. If the reference material is thermally inert, the heating rate will be the same throughout the sample after quasi-steady state conditions have been established. Equation 6 is thus valid for any sample shape.

TEMPERATURE OF MAXIMUM DEFLECTION

Most reactions of the type solid → solid + gas can be described by an equation

$$\frac{dx}{dt} = A(1-x)^n e^{-\frac{E}{RT}} \qquad (7)$$

where dx/dt is the rate, x is the fraction reacted, n is the empirical order of reaction, and T is the Kelvin temperature.

Reactions of this type may take place by one of a number of elementary mechanisms, as well as combinations of these mechanisms. In most cases which have been studied, the exponent n in Equation 7 is unity or fractional, and remains constant through the greater part of the reaction. The results of studies of solid decomposition mechanisms are summarized by Garner (*4*). In the present paper it is assumed that n remains constant.

Analytical solution for the Kissinger equation

Pere Roura[a] and Jordi Farjas
Grup de Recerca en Materials i Termodinamica (GRMT), Department of Physics, University of Girona, Campus Montilivi, E17071 Girona, Catalonia, Spain

(Received 25 March 2009; accepted 29 June 2009)

An analytical solution for the Kissinger equation relating the activation energy, E, with the peak temperature of the reaction rate, T_m, has been found. It is accurate (relative error below 2%) for a large range of E/RT_m values (from 15 to above 60) that cover most experimental situations. The possibilities opened by this solution are outlined by applying it to the analysis of some particular problems encountered in structural relaxation of amorphous materials and in kinetic analysis.

I. INTRODUCTION

When the rate of a reaction is governed by a single limiting step, the evolution with time of the conversion degree, α, is described by a differential equation of the form[1]:

$$\frac{d\alpha}{dt} = f(\alpha)k(T) \quad , \tag{1}$$

where $f(\alpha)$ depends on the type of rate-controlling process and $k(T)$ is the temperature-dependent rate constant. Usually, $k(T)$ follows an Arrhenius dependence:

$$k(T) = A_k e^{-E/RT} \quad , \tag{2}$$

where A_k is constant, E is the activation energy, T the temperature, and R the gas constant. When the temperature varies with time, Eq. (1) still holds for spatially homogeneous reactions, whereas for heterogeneous reactions such as crystallization it is only approximate.[2] The most common nonisothermal experiments involve constant heating conditions, i.e.,

$$T = T_0 + \beta t \quad , \tag{3}$$

where T_0 is chosen low enough to have a negligible effect on the results. These kinds of experiments allow A_k and E to be determined provided that a particular kinetics $[f(\alpha)]$ is assumed.

Despite the large number of kinetic models, there is a simple relationship between the kinetic parameters, E and A_k, and the temperature, T_m, at which the transformation rate is at its maximum. Namely,

$$\frac{E}{RT_m^2} = \frac{A}{\beta} e^{-E/RT_m} \quad . \tag{4}$$

A is equal to A_k for most kinetics or is proportional to it.[3] This equation was first derived by Kissinger.[4] It is widely used for the analysis of structural transformations as diverse as the dehydrogenation of carbon nanotubes,[5] the crystallization of glasses,[6,7] and the thermal analysis of lipids, proteins, and biological membranes,[8] because the slope of $\mathrm{Ln}(\beta/T_m^2)$ versus $1/RT_m$ (Kissinger plot) is just the activation energy. It is exact only for first-order kinetics [$f(\alpha) = 1-\alpha$],[9] and it is accurate for other kinetics provided that E/RT_m is large enough (for most kinetics, the error in E is lower than 2% if $E/RT_m > 10$).[9] A literature review reveals that this does not represent a serious limitation to the applicability of Eq. (4): (i) $E/RT_m > 25$ for most glass-crystal transformations[10] and (ii) we have found values in the 8 to 35 range in reactions involving polymers[11] and thermal decomposition of molecules[5,12] (among them, values below 10 are scarce).

Until now, the Kissinger Eq. (4) has mainly been used for the analysis of experimental data through the popular Kissinger plot. Using this equation to find the analytical relationship between the parameters involved in a given reaction is not straightforward because the Kissinger equation itself lacks an exact analytical solution. In this work, we will show that within the range $15 < E/RT_m < 60$, which covers most experimental situations, an accurate analytical solution can be used. To illustrate the interest in this solution, several applications are detailed at the end of this work. Most of them have proven useful in a paper recently published by us.[13] We should make clear here that our analytical solution is not intended for use instead of the Kissinger equation itself in the analysis of experimental data, where the use of the Kissinger plot is adequate. The examples at the end of the work indicate that its natural applications are in theoretical analyses.

II. THE ANALYTICAL SOLUTION

The Kissinger Eq. (4) can be rewritten in terms of the reduced activation energy, $x \equiv E/RT$, and the reduced pre-exponential rate constant, AT_m/β, as

[a]Address all correspondence to this author.
e-mail: pere.roura@udg.es
DOI: 10.1557/JMR.2009.0366

$$x_{\mathrm{m}} = \mathrm{Ln}\left(\frac{AT_{\mathrm{m}}}{\beta}\right) + \mathrm{Ln}\left(\frac{1}{x_{\mathrm{m}}}\right) \quad . \tag{5}$$

A plot of x_{m} versus $\mathrm{Ln}(AT_{\mathrm{m}}/\beta)$ (inset of Fig. 1) reveals a quasilinear dependence with a slope close to 1 for the useful x_{m} range of most solid state reactions (i.e., $15 < x_{\mathrm{m}} < 60$). This simple dependence arises because of the reduced variation of x_{m} when AT_{m}/β spans over many orders of magnitude (see inset of Fig. 1). Consequently, an approximate analytical solution of Eq. (4) can be written as

$$x_{\mathrm{m}} = \mathrm{Ln}\left(\frac{AT_{\mathrm{m}}}{\beta}\frac{1}{x_{\mathrm{m0}}}\right) \quad , \tag{6}$$

where x_{m0} is a particular value between 15 and 60. The accuracy of this solution has been tested for several values of x_{m0} and the relative error in the whole range has been plotted in Fig. 1. Relative errors below 2% are achieved with $x_{\mathrm{m0}} = 20$. These are also the relative errors of the activation energy, when Eq. (6) is solved for E:

$$E = \mathrm{R}T_{\mathrm{m}}\mathrm{Ln}\left(\frac{AT_{\mathrm{m}}}{\beta}\frac{1}{x_{\mathrm{m0}}}\right) \quad , \tag{7}$$

and, when solved for T_{m},

$$\frac{1}{T_{\mathrm{m}}} = \frac{\mathrm{R}}{E}\mathrm{Ln}\left(\frac{A}{\beta}\frac{E}{\mathrm{R}}\frac{1}{{x_{\mathrm{m0}}}^2}\right) \quad , \tag{8}$$

the relative errors are twice those of E, because x_{m0} now appears squared. Of course, the accuracy can be improved if the range of x_{m} is restricted and x_{m0} is chosen inside the range. The accuracy achieved for E is higher than that obtained from most experiments. In addition, it is similar to the accuracy of the Kissinger equation itself when applied to the analysis of non-first-order kinetics.[9] Consequently, although Eqs. (6)–(8) are not exact, they are accurate enough to be used in theoretical analyses involving the Kissinger equation. Some examples are given in Sec. III.

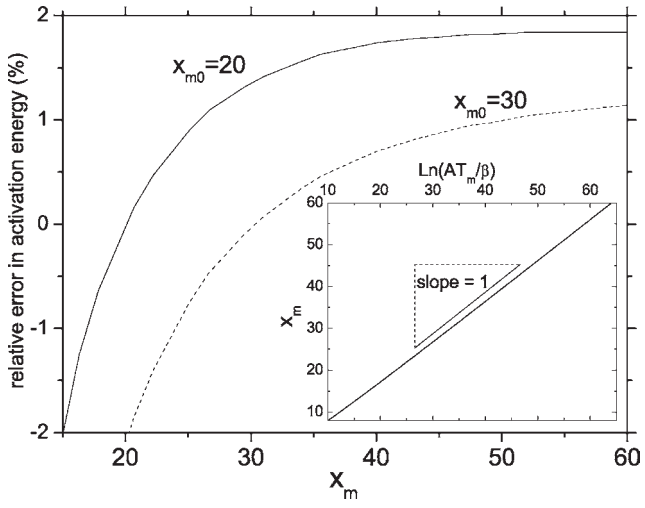

FIG. 1. Relative error in the activation energies delivered by the analytical solution [Eq. (7)] with a single value of x_{m0} for the entire range of interest of x_{m}. Inset: exact solution of the Kissinger equation.

III. SOME APPLICATIONS

The first two examples concern structural relaxation processes in amorphous materials. These processes cannot be directly described by Eq. (1), because they are not governed by single activation energy. Consequently, analysis of the transformation temperature shift with the heating rate through the Kissinger equation can lead to erroneous interpretation of the activation energy.[14]

It is usually accepted that structural relaxation involves a distribution of independent defects that relax to a lower energy state.[15] A particular kind of defect is identified by its activation energy and many analyses consider that the pre-exponential rate constant is the same for all defects.[16,17] Therefore, structural relaxation can be formally described by the superposition of a continuum of transformations characterized by a distribution of activation energies, $N(E)$. Any particular transformation will follow Eq. (1) and will obey the Kissinger equation.[13] Under these assumptions, a simple relationship can be found between the peak temperature of a given transformation within the distribution and its activation energy. The derivative of Eq. (7) in T_{m} leads to

$$\delta T_{\mathrm{m}} = \frac{\delta E/\mathrm{R}}{\mathrm{Ln}\left(\frac{AT_{\mathrm{m}}}{\beta}\frac{1}{x_{\mathrm{m0}}}\right) + 1} = B\delta E \quad , \tag{9}$$

where B is almost constant (almost independent of T_{m}) for a given heating rate. In other words, although for relaxation experiments at a constant heating rate it is more natural to describe the defects by the distribution of peak temperature; this distribution has a shape that is nearly identical to the distribution of activation energies. Additionally, B has a smooth dependence on the heating rate. For the particular case of structural relaxation of a-Si (take $\mathrm{A} \approx 10^{13}\ \mathrm{s}^{-1}$, the Debye frequency),[16] B increases by 20% when β increases from the usual values of conventional differential scanning calorimetry (1 K/s) to the high values of nanocalorimetry (10^4 K/s).[18]

Concerning the activation energy of the defects in the distribution, we will show that, for constant A, it is almost proportional to the peak temperature. Without any further approximation, application of Eq. (7) to (E_1, T_{m1}) and (E, T_{m}) leads to:

$$E = \frac{E_1}{T_{\mathrm{m1}}}T_{\mathrm{m}}\left[1 + \frac{1}{x_{\mathrm{m1}}}\mathrm{Ln}\left(\frac{T_{\mathrm{m}}}{T_{\mathrm{m1}}}\right)\right] \approx \frac{E_1}{T_{\mathrm{m1}}}T_{\mathrm{m}} \quad , \tag{10}$$

where the last expression is obtained because $x_{\mathrm{m1}} >> 1$. Of course, the higher x_{m1} the better the proportionality between T_{m} and E. Thanks to this relationship, we have shown in Ref. 13 that, when A is constant, the logarithmic

variations with time of selected properties during the isothermal relaxation of amorphous materials have a slope proportional to the annealing temperature.

The next two examples have a general interest in kinetic analysis. First of all, we will derive a relationship that allows calculating the shift of T_m when the heating rate is increased from β_1 to β_2. From Eq. (8) we obtain the exact formula (x_{m0} replaced by x_{mi}):

$$\Delta(1/T_m) \equiv \frac{1}{T_{m2}} - \frac{1}{T_{m1}} = \frac{R}{E}[\mathrm{Ln}(\beta_1/\beta_2) + 2\mathrm{Ln}(x_{m1}/x_{m2})] \quad . \tag{11}$$

Since, as commented previously, x_m has a variation smoother than that of β (in fact $\beta R/AE$), we can expand the logarithm of x_{mi} around $x_{m1}/x_{m2} = 1$ (i.e., around $T_{m2}/T_{m1} = 1$). We obtain

$$\Delta(1/T_m) = \frac{R}{E}\left[\mathrm{Ln}(\beta_1/\beta_2) - 2\frac{\Delta(1/T_m)}{1/T_{m1}}\right] \quad . \tag{12}$$

Solving for $\Delta(1/T_m)$ leads us to the desired result:

$$\Delta(1/T_m) \approx \frac{1}{T_{m1}}\frac{\mathrm{Ln}(\beta_1/\beta_2)}{2 + x_{m1}} \quad . \tag{13}$$

A similar, less accurate relationship was published several decades ago.[19] Numerical analysis of our approximate relationship reveals that, as expected, its accuracy improves when x_m becomes higher. Consider the particular case of a process with peak temperature T_m = 500 K and activation energy of 83.1 KJ/mol (x_m = 20). When the heating rate is increased by a factor of 100, Eq. (13) predicts a shift of the peak temperature of 132.4 K, which is very close to the exact result of 130.6 K.

Finally, we will consider second-order kinetics. This is the kinetics governing defect recombination in crystalline materials. Their concentration, C, diminishes according to a bimolecular reaction:

$$\frac{dC}{dt} = -k_C C^2 \quad , \tag{14}$$

where k_C is thermally activated. With the definition of the transformed fraction as

$$\alpha \equiv \frac{C_0 - C}{C_0} \quad , \tag{15}$$

where C_0 is the initial concentration, we arrive to the particular form of Eq. (1) for a second-order reaction

$$\frac{d\alpha}{dt} = (k_C C_0)(1-\alpha)^2 \quad , \tag{16}$$

that, compared with Eqs. (1) and (2), leads to the conclusion that the reaction rate $k(T)$ is proportional to C_0. This means, according to our analytical solution of the Kissinger equation [Eq. (8)], the peak temperature will depend on C_0 through the pre-exponential constant A. When the initial concentration changes from C_{01} to C_{02}, the shift of the peak temperature can be deduced, as we have done for the previous application and we obtain

$$\Delta(1/T_m) \approx \frac{1}{T_{m1}}\frac{\mathrm{Ln}(C_{02}/C_{01})}{2 + x_{m1}} \quad . \tag{17}$$

This last formula has been applied in Ref. 13 to show that in amorphous materials structural relaxation cannot be described by a superposition of second-order recombination processes.

IV. CONCLUSIONS

To conclude, we can say that during the past 50 years, the Kissinger equation has been widely used for the analysis of experiments concerning the kinetics of structural transformations. Despite this success, the particular functional dependencies on E and T_m make it difficult to use the equation for general analytical predictions. Instead, predictions involve solving the equation numerically for particular conditions. We hope that the analytical solution obtained in this work will broaden the range of applications of the Kissinger equation.

ACKNOWLEDGMENT

This work was supported by the Spanish Programa Nacional de Materiales under Contract No. MAT2006-11144.

REFERENCES

1. D.W. Henderson: Thermal-analysis of nonisothermal crystallization kinetics in glass forming liquids. *J. Non-Cryst. Solids* **30,** 301 (1979).
2. J. Farjas and P. Roura: Modification of the Kolmogorov-Johnson-Mehl-Avrami rate equation for non-isothermal experiments and its analytical solution. *Acta Mater.* **54,** 5573 (2006).
3. J. Farjas and P. Roura: Simple approximate analytical solution for nonisothermal single-step transformations: Kinetic analysis. *AIChE J.* **54,** 2145 (2008).
4. H.E. Kissinger: Reaction kinetics in thermal analysis. *Anal. Chem.* **29,** 1702 (1957).
5. J.W. Lee, H.S. Kim, J.Y. Lee, and J.K. Kang: Hydrogen storage and desorption properties of Ni-dispersed carbon nanotubes. *Appl. Phys. Lett.* **88,** 143126 (2006).
6. E. Jona, P. Simon, K. Nemcekova, V. Pavlik, G. Rudinska, and E. Rudinska: Thermal properties of oxide glasses. Part II. Activation energy as a criterion of thermal stability of $Li_2O{\cdot}2SiO_2{\cdot}nTiO_2$ glass systems against crystallization. *J. Therm. Anal. Calorim.* **84,** 673 (2006).
7. A.P. Srivastava, D. Srivastava, and G.K. Dey: A study on microstructure, magnetic properties and kinetics of the nanocrystallization of $Fe_{40}Ni_{38}B_{18}Mo_4$ metglass. *J. Magn. Magn. Mater.* **306,** 147 (2006).
8. B.D. Ladbrook and D. Chapman: Thermal analysis of lipids, proteins and biological membranes. A review and summary of some recent studies. *Chem. Phys. Lipids* **3,** 304 (1969).

9. P. Budrugeac and E. Segal: Applicability of the Kissinger equation in thermal analysis revisited. *J. Therm. Anal. Calorim.* **88,** 703 (2007).
10. H. Yinnon and D.R. Uhlmann: Applications of thermoanalytical techniques to the study of crystallization kinetics in glass-forming liquids. 1. Theory. *J. Non-Cryst. Solids* **54,** 253 (1983).
11. S. Vyazovkin and N. Sbirrazzuoli: Isoconversional kinetic analysis of thermally stimulated processes in polymers. *Macromol. Rapid Commun.* **27,** 1515 (2006).
12. S.K. Padhi: Solid-state kinetics of thermal release of pyridine and morphological study of $[Ni(ampy)_2(NO_3)_2]$; ampy = 2-picolylamine. *Thermochim. Acta* **448,** 1 (2006).
13. P. Roura and J. Farjas: Structural relaxation kinetics for first and second-order processes: Application to pure amorphous silicon. *Acta Mater.* **57,** 2098 (2009).
14. V.A. Khonik, K. Kitagawa, and H. Morii: On the determination of the crystallization activation energy of metallic glasses. *J. Appl. Phys.* **87,** 8440 (2000).
15. M.R.J. Gibbs, J.E. Evetts, and J.A. Leake: Activation-energy spectra and relaxation in amorphous materials. *J. Mater. Sci.* **18,** 278 (1983).
16. J.H. Shin and H.A. Atwater: Activation-energy spectrum and structural relaxation dynamics of amorphous-silicon. *Phys. Rev. B* **48,** 5964 (1993).
17. W. Deceuninck, G. Knuyt, H. Stulens, L. Deschepper, and L.M. Stals: Determination of the attempt frequency for relaxation phenomena in amorphous metals. *Mater. Sci. Eng., A* **133,** 337 (1991).
18. J-F. Mercure, R. Karmouch, Y. Anahory, S. Roorda, and F. Schiettekatte: Dependence of the structural relaxation of amorphous silicon on implantation temperature. *Phys. Rev. B* **71,** 134205 (2005).
19. C. Popescu and E. Segal: Variation of the maximum rate of conversion and temperature with heating rate in non-isothermal kinetics. 2. *Thermochim. Acta* **82,** 387 (1984).

Netsu Sokutei **20**(4)210-223

総　説

Data Treatment in Non-isothermal Kinetics and Diagnostic Limits of Phenomenological Models

Nobuyoshi Koga*, Jiri Malek**, Jaroslav Sestak*** and Haruhiko Tanaka*

(received April 19, 1993)

* Chemistry Laboratory, Faculty of School Education,
Hiroshima University, 3-1-33
Shinonome, Minami-Ku, Hiroshima 734, Japan.
** Joint Laboratory of Solid State Chemistry,
Academy of Sciences of the Czech Republic and University Chemical Technology,
Studentska 84, CR-530 09 Pardubice, Czech Republic.
*** Division of Solid State Physics, Institute of Physics,
Academy of Sciences of the Czech Republic.
Cukrovarnicka 10, CR-162 00 Prague 6, Czech Republic.

Kinetic models of solid-state reactions are often based on a formal description of geometrically well defined bodies treated under strictly isothermal conditions; for real processes these assumptions are evidently incorrect. The kinetic parameters are distorted by the difference of the real process from the idealized kinetic model. In this respect, it can be useful to find an empirical function containing the smallest possible number of constants, so that there is some flexibility enough to describe real process as closely as possible. In such a case the models of heterogeneous kinetics can be assumed as a distorted case of the simpler homogeneous kinetics and then mathematically treated by multiplying an "accommodation" function. The empirical function also accommodates the deviation of the non-isothermal process from the process under the isothermal condition. The mutual dependence of the Arrhenius parameters observed empirically is recognized as a simple mathematical consequence of the exponential form of the rate constant in the Arrhenius equation, resulting from both the poorly controlled measuring condition in the thermal analysis and the false kinetic treatment. The isoconversion method allows to check the invariance of the activation energy during the course of reaction, which is the fundamental assumption in the derivation of the kinetic equation. Once the characteristic activation energy is determined, it is possible to find the kinetic model function which best describes the measured set of TA data using the two special functional relationships in the kinetic equation.

Introduction

In contradiction to the well established spot measurements frequently employed to investigate solid-state reactions, although affected by inadequate freeze-in and poor localization of the reaction, the centered measurements of a property representing the average state of a sample are often considered less convenient due to superstitiously bad reputation of its mere phenomenological character. The latter

group is represented by methods of thermal analysis (TA) carried out under constant heating and/or cooling. TA curves are often treated in terms of homogeneous-like kinetic description yielding non-integral values of reaction orders which are almost meaningless in heterogeneous kinetics. However, even the homogeneous reactions exhibiting nonrandomness of the reactant distribution and/or diffusion controlled subprocess can be described by reactions on fractal domains, the hallmark being the anomalous reaction orders. It is clear that the present state-of-art of the thermoanalytical kinetics[1] as applied to heterogeneous reactions is not appropriate to sophisticated means available in solid-state chemistry, the linkage of most treatments to the traditional geometrical description being very firm and hard to overcome[1-3]. The use of phenomenological models has been criticized[2] but a unified approach is still missing as well as the correlation between the microscopic process (detectable only locally under not well guaranteed conditions) and macroscopic process (capable of measuring in situ even at changing temperatures). With gradual increment of complexity of an experimentally resolved kinetic curve from TA measurement of the reaction investigated, the kinetic approach tends to be mere distinguishment of the proportional relevancy of the individual groups of phenomenological models. Important is the discussion on the applicability and limitation of the kinetic analysis of non-isothermal data.

In this article, the present orthodoxy of the kinetic study of the solid-state reactions by means of TA is reviewed briefly. Some problems, resulting from the distortion of the real reaction process detected by TA measurements from the ideal case assumed to formulate the kinetic equation, are pointed out in connection with some consequence of the mutual correlation of the kinetic parameters and their implications for a reliable kinetic analysis. A possible way to accommodate such a deviation in the kinetic equation is discussed by introducing the accommodation function $a(\alpha)$[4]. The significance of an empirical kinetic model function known as the Sestak-Berggren (SB) model is investigated in relation to $a(\alpha)$. Taking account of these findings, two types of mathematical relationships useful to characterize the kinetics are reviewed.

The Kinetic Equation

Assuming the kinetic model function $f(\alpha)$ and the Arrhenius type of temperature dependence of the rate constant, the following equation is applied for analyzing kinetically the TA curves of the solid-state reaction[3].

$$\frac{d\alpha}{dt} = A\exp(-\frac{E}{RT})f(\alpha) \qquad (1)$$

where A and E are the Arrhenius parameters and α is the fractional conversion. The kinetic model function $f(\alpha)$ is derived on the basis of physico-geometric assumptions on the movement of reaction interface. Figure 1 represents a schematic diagram of a hypothetical transfer of the geometry of the system from the dimensionless homogeneous-like model to the idealized heterogeneous model by introduction of dimensionality. It is important to recall that character of kinetic description drastically changes from the concentration dependent (homogeneous) to that of the interface-to-volume dependent (heterogeneous). The mathematical formulae of the commonly cited $f(\alpha)$ are summarized in Table 1.

Because the rate constant is characteristic for the $f(\alpha)$ assumed, the Arrhenius parameters are mutually correlated with the $f(\alpha)$. As a simple mathematical consequence of the exponential form of the rate constant, the distortion of the Arrhenius parameters by the inappropriate kinetic model function is expressed by [5]

$$\frac{E_{app}}{E} = \frac{f(\alpha_p)F'(\alpha_p)}{F(\alpha_p)f'(\alpha_p)} \qquad (2)$$

with $f'(\alpha)=df(\alpha)/d\alpha$ and $F'(\alpha)=dF(\alpha)/d\alpha$, and

$$\ln\frac{A_{app}}{A} = \frac{E}{RT_p}\left[\frac{f(\alpha_p)F'(\alpha_p) - F(\alpha_p)f'(\alpha_p)}{F(\alpha_p)f'(\alpha_p)}\right] + \ln\frac{f(\alpha_p)}{F(\alpha_p)} \qquad (3)$$

where E_{app} and A_{app} are the apparent Arrhenius parameters distorted by the use of an inappropriate model $F(\alpha)$ instead of the appropriate one $f(\alpha)$. The subscript p indicates the values correspond to the

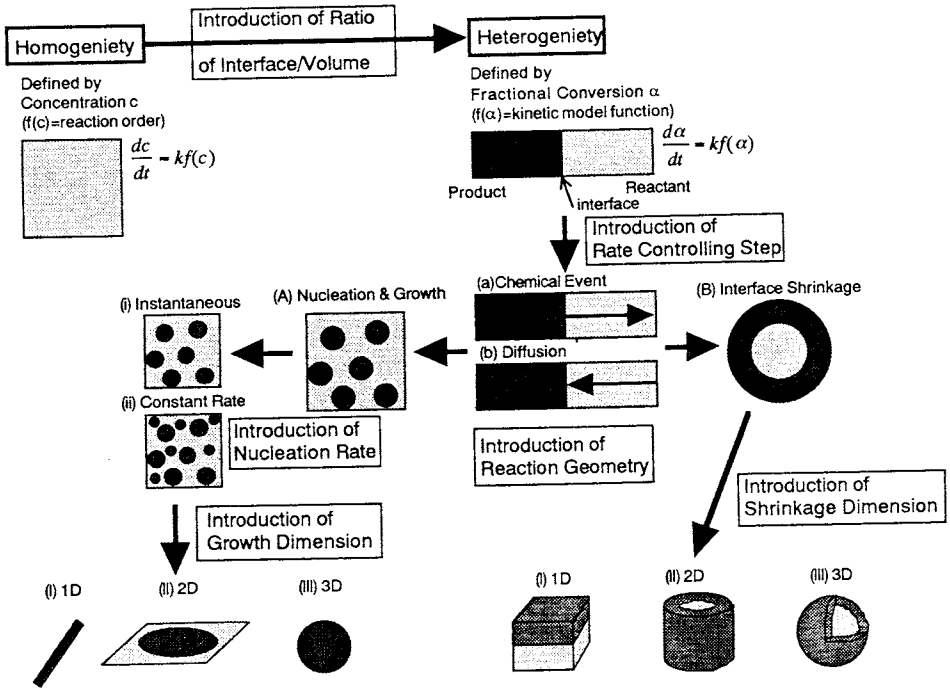

Fig.1 Schematic diagram of a hypothetical transfer of the system geometry from the non-dimensional homogeneous-like model to the idealized heterogeneous model by introduction of dimensionality, due to the interface formation and interface growth.

Table 1 The kinetic model functions $f(\alpha)$ usually employed for the kinetic analysis of the solid-state reaction, together with their integral $g(\alpha)$ and differential $f'(\alpha)$ forms.

Model	Symbol	$f(\alpha)$	$g(\alpha)=\int_0^\alpha \frac{d\alpha}{f(\alpha)}$	$f'(\alpha)=\frac{f(\alpha)}{d\alpha}$
Nucleation & Growth (Avrami-Erofeyev)	A_m (m = 0.5, 1, 1.5, 2, 2.5, 3 and 4)	$m(1-\alpha)[-\ln(1-\alpha)]^{1-1/m}$	$[-\ln(1-\alpha)]^{1/m}$	$\frac{m-1}{[-\ln(1-\alpha)]^{1/m}} - \frac{m}{[-\ln(1-\alpha)]^{1/m-1}}$
Phase Boundary Controlled Reaction	R_n (n = 1, 2 and 3)	$n(1-\alpha)^{1-1/n}$	$1-(1-\alpha)^{1/n}$	$-\frac{n-1}{(1-\alpha)^{1/n}}$
One-dimensional Diffusion	D_1	$\frac{2}{\alpha}$	α^2	$-\frac{2}{\alpha^2}$
Two-dimensional Diffusion	D_2	$-\frac{1}{\ln(1-\alpha)}$	$\alpha+(1-\alpha)\ln(1-\alpha)$	$-\frac{1}{(1-\alpha)[\ln(1-\alpha)]^2}$
Three-dimensional Diffusion (Jander)	D_3	$\frac{3(1-\alpha)^{2/3}}{2[1-(1-\alpha)^{1/3}]}$	$[1-(1-\alpha)^{1/3}]^2$	$\frac{1/2-(1-\alpha)^{-1/3}}{[1-(1-\alpha)^{1/3}]^2}$
Three-dimensional Diffusion (Ginstring-Brounshtein)	D_4	$\frac{3}{2[(1-\alpha)^{-1/3}-1]}$	$1-\frac{2\alpha}{3}-(1-\alpha)^{2/3}$	$-\frac{1}{2(1-\alpha)^{4/3}[(1-\alpha)^{-1/3}-1]^2}$

maximum of the TA peak.

In practice, if the reaction order $RO(N)$ model, $(1-\alpha)^N$, was used instead of the appropriate kinetic model function $f(\alpha)$, the ratio of the apparent and the true activation energies E_{app}/E can be expressed by the following equation[5]:

$$\frac{E_{app}}{E} = -\left(\frac{f(\alpha_p)}{f'(\alpha_p)}\right)\frac{N_{app}}{1-\alpha_p} \qquad (4)$$

where N_{app} is an apparent kinetic exponent of the $RO(N)$ model, The value of N_{app} is characteristic for the $f(\alpha)$ but α_p depends also on the $x_p=E/RT_p$. Therefore the value of E_{app}/E sightly increases with increasing x_p for the $f(\alpha)$ of diffusion controlled models[6]. On the other hand, the E_{app}/E ratio decreases with increasing x_p for the A_m model according to the equation[7]:

$$\frac{E_{app}}{E} = \frac{m-1}{x_p\pi(x_p)} + 1 \qquad (5)$$

where m is the true kinetic exponent of the A_m model and $\pi(x)$ is the approximation of the temperature integral[3].

It should be emphasized that many workers are concerned with the kinetic analysis of a single TA curve. However, the methods are somewhat problematic because of the apparent kinetic models. For example the popular Freeman and Carroll method[8] was derived for the $RO(N)$ model. Therefore, this method always gives apparent parameters N_{app} and E_{app} corresponding to the $RO(N)$ model regardless of the true kinetic model. Similarly it must be borne in mind, that the non-linear or multiple linear regression methods can lead to incorrect results because any TA curve can be interpreted within the scope of the $RO(N)$ model depending on the value of apparent activation energy.

Accommodation Function and Empirical Kinetic Model

Figure 2 represent a typical polarizing microscopic view of internal surfaces of partially dehydrated crushed crystals of $K_2CuCl_4 \cdot 2H_2O$. The irregularly shaped sample particles and reaction interfaces are apparently different from the idealized $f(\alpha)$. In addition, the behavior of real particles does require to account for polydispersity, shielding and overlapping, unequal mixing, anisotropy and so on, as is shown schematically in Fig.3. The kinetic model functions $f(\alpha)$ derived on the basis of physico-geometric assumptions of regularly shaped bodies evidently can hardly describe such a real heterogeneous system which we have to take into consideration. The disagreement between the idealized process, assumed in formulating the $f(\alpha)$, and the actual process, investigated as an averaged phenomena by the TA measurements, leads to the distortion of the Arrhenius parameters according to eqns. (2) and (3).

Fig.2 Typical polarizing microscopic view of the internal surface of the partially dehydrated crushed crystals of $K_2CuCl_4 \cdot 2H_2O$.

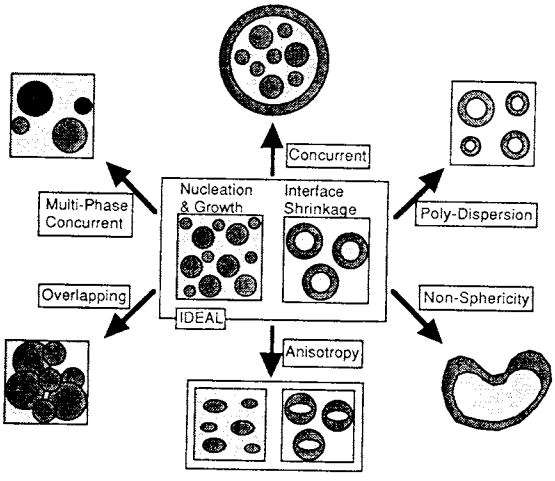

Fig.3 Schematic diagram of the practical reaction processes.

Table 2 The kinetic model functions $h(\alpha)$ with the non-integral kinetic exponent and the accommodation function $a(\alpha)$, together with their physico-chemical meanings.

$f(\alpha)$	Kinetic exponent of interface advancement	Dimentionality	Kinetic exponent of nucleation	$h(\alpha)$	$a(\alpha)$
R_n	1	fractal value N	---	$N(1-\alpha)^{1-1/N}$	$\frac{N}{n}(1-\alpha)^{(N-n)/nN}$
R_3	non-integral value p	3	---	$\frac{3(1-\alpha)^{2/3}}{p[1-(1-\alpha)^{1/3}]^{p-1}}$	$\frac{1}{p[1-(1-\alpha)^{1/3}]^{p-1}}$
R_n	non-integral value p	fractal value N	---	$\frac{N(1-\alpha)^{1-1/N}}{p[1-(1-\alpha)^{1/N}]^{p-1}}$	$\frac{N(1-\alpha)^{(N-n)/nN}}{n\,p[1-(1-\alpha)^{1/N}]^{p-1}}$
D_3	2	fractal value N	---	$\frac{N(1-\alpha)^{1-1/N}}{2[1-(1-\alpha)^{1/N}]}$	$\frac{N}{3}(1-\alpha)^{(N-3)/3N}$
A_m	non-integral value	fractal value	non-integral value	$M(1-\alpha)[-\ln(1-\alpha)]^{1-1/M}$	$\frac{M}{m}[-\ln(1-\alpha)]^{(M-m)/mM}$

Introducing the accommodation function $a(\alpha)$, the discrepancy of the idealized $f(\alpha)$ from the actual kinetic model function $h(\alpha)$ can be expressed as[4]:

$$h(\alpha)=f(\alpha)a(\alpha) \tag{6}$$

Then the kinetic expression $h(\alpha)$ can be regarded as the distorted case of the homogeneous-like kinetics and of $f(\alpha)$, with a possible $a(\alpha)$ to decrease the difference of the idealized $f(\alpha)$ from the practial process. Mathematical formalism of the $a(\alpha)$ is possible for a certain case. The simplest example of the accommodation is the application of the non-integral kinetic exponents into the $f(\alpha)$. Table 2 lists the form of $a(\alpha)$ for the $h(\alpha)$ having the non-integral exponents, together with their physico-geometric meaning[9]. Although the reaction geometry is also influenced by the extensive factors, from the simple geometric consideration the non-integral exponent is taken as the value corresponding fractal dimension[10].

It is apparent, however, that the accommodation of the more complicated process in the $h(\alpha)$ is extremely difficult based on the real physical chemistry and is possibly expressed by the empirical (analytical) formula. The validity of procedures and resulting functions in deriving kinetic models in question was approved also for non-isothermal conditions elsewhere[11),12)]. From this point of view it would be useful to find an empirical function $h(\alpha)$ containing the smallest possible number of constants, so that there is some flexibility enough to describe real TA data as closely as possible[3]. Twenty years ago, Sestak and Berggren[13] proposed an empirical kinetic model in the form

$$h(\alpha)=\alpha^m(1-\alpha)^n[-\ln(1-\alpha)]^r \tag{7}$$

It was believed[2),3)] that this kinetic equation, containing as many as three exponential terms, is able to describe any TA curves. Further mathematical analysis[14] of eqn. (7) has shown, however, that no more than two kinetic exponents are necessary. Therefore, after eliminating the third exponential term in eqn. (7) the final form obtained is

$$h(\alpha)=\alpha^m(1-\alpha)^n \tag{8}$$

In the literature the eqn. (8) is cited as the Sestak Berggren $SB(m,n)$ kinetic model. Exponents m and n are taken as kinetic parameters which describe the shape of measured TA curves. The SB model, eqn. (7), can also be understood in terms of the $a(\alpha)$, where $a(\alpha)$ can bear the form of either function, α^m, $(1-\alpha)^{1-n}$ and/or $[-\ln(1-\alpha)]^r$. It serves particularly to fit the prolonged reaction tails due to the actual

Table 3 Typical empirical kinetic model functions $h(\alpha)$, together with their integral form $G(\alpha)$and differential form $h'(\alpha)$.

Type	Symbol	$h(\alpha)$	$G(\alpha)=\int_0^\alpha \frac{d\alpha}{h(\alpha)}$	$h'(\alpha)=\frac{h(\alpha)}{d\alpha}$
Reaction order	*RO(N)*	$(1-\alpha)^N$	$\frac{1-(1-\alpha)^{1-N}}{1-N}$	$-N(1-\alpha)^{N-1}$
Johnson-Mehl-Avrami-Erofeyev	*JMA(M)*	$M(1-\alpha)[-\ln(1-\alpha)]^{1-1/M}$	$[-\ln(1-\alpha)]^{1/M}$	$\frac{M-1}{[-\ln(1-\alpha)]^{1/M}}-\frac{M}{[-\ln(1-\alpha)]^{1/M-1}}$
Sestak-Berggren	*SB(m,n)*	$\alpha^m(1-\alpha)^n$	no analytical form	$m\alpha^{m-1}(1-\alpha)^n-n\alpha^m(1-\alpha)^{n-1}$

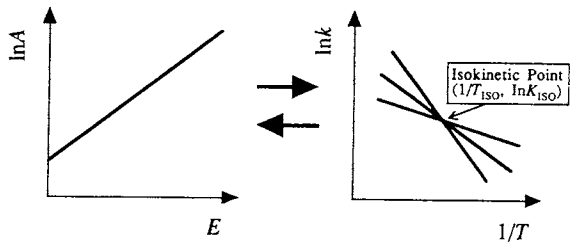

Fig.4 Schematic representation of the mutual dependence of the Arrhenius parameters.

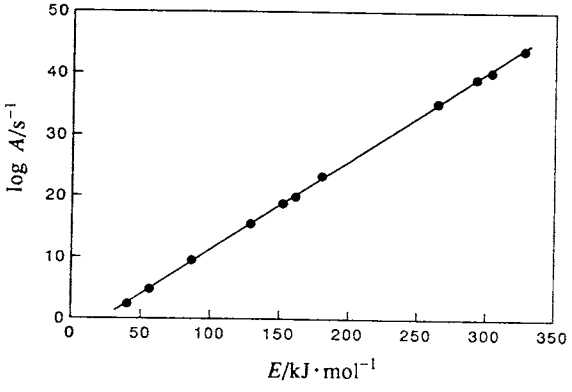

Fig.5 The kinetic compensation behavior of the apparent Arrhenius parameters obtained using various inappropriate f(α) for a theoretical curve drawn by assuming E=150 kJ/mol, log A=18.5 1/s, Heating Rate=0.5 K/min and the R_2 law.

behavior of real particles and can match the particle non-sphericity in view of the morphology description in terms of the characteristic dimensions (usually the longest particle length), interface (the average boundary line) and volume (the mean section area). Table 3 lists the typical empirical model $h(\alpha)$, together with their integral and differential forms.

Correlation of the Arrhenius Parameters

It is rather an empirical fact that both the activation energy and preexponential factor in eqn. (1) are mutually correlated known as the kinetic compensation effect (KCE)[15]. This correlation can be expressed by the following equation.

$$\ln A = a + bE \tag{9}$$

where a and b are constants. Any change in the activation energy is therefore "compensated" by the change of ln$A$ as expressed by eqn.(9). The simple relationship of eqn. (9) can be derived as a mathematical consequence of the exponential form of the rate constant in the Arrhenius equation[16] and seems to arise from a projection of the interrelationship among ln$A$, E and temperature, T, terms to the ln$A$ vs. E coordinate[17], see Fig.4. From this point of view, the KCE can be divided into two categories according to whether the KCE is accompanied by changes in the temperature interval analyzed or not[18].

As described in the previous section, the KCE arising from a single non-isothermal TA curve by the use of various inappropriate kinetic model

functions is one of the examples where the T terms remain constant[5]. As an example, Figure 5 shows the KCE behavior of the apparent Arrhenius parameters obtained using various inappropriate $f(\alpha)$ for a theoretical cuve drawn by assuming E=150 kJ/mol, log A=18.5 1/s, Hearing Rate=0.5 K/min and R_2 law. It seems, therefore, problematic to obtain all the kinetic parameters from only one experimental TA curve. Similarly, we have to realize that this problem cannot be solved even using the most sophisticated non-linear regression algorithms unless the kinetic model or at least one kinetic parameter is a *priori* known.

On the other hand, in the case of a KCE established between the Arrhnius parameters obtained from more than one TA curve under various sample and measuring conditions, the changes in the values of E and ln$A$ are always accompanied by a change in the working temperature interval of kinetic analysis[19]. For the values of E_{app} and A_{app}, the following relationships can be derived by using the lowest temperature, T_L, the highest temperature, T_H, and $\Delta T=T_H-T_L$

$$E_{app}=\frac{RT_HT_L}{\Delta T}\ln X \tag{10}$$

$$\ln A_{app}=\frac{1}{T_{iso}}\frac{T_HT_L}{\Delta T}\ln X+\ln k_{iso} \tag{11}$$

where X depends on the calculation method. Table 4 lists the form of X for the respective method of kinetic calculation. The variation in the value of ln$X$ due to the different reaction temperatures is relatively small compared with the change in the value of $T_HT_L/\Delta T$. This implies that a constant value of $T_HT_L/\Delta T$ is a necessary condition for obtaining a constant E_{app} value[20]. In this case, however, a constant value of ln$A$ is not necessarily obtained; the constant value of ΔT can yield constant Arrhenius parameters. This is explained that, for a smaller ΔT, even the change in T_HT_L can be ignored in comparison with the change in $1/\Delta T$. When the KCE is established among several sets of Arrhnius parameters, the values of E_{app} and ln A_{app} are to be a function of $1/\Delta T$. Figure 6 represents the practical example of the $1/\Delta T$ dependence of the apparent E values obtained at different α for the nonisothermal dehydration of single crystalline $Li_2SO_4\cdot H_2O$.

Such a change in the working temperature interval, which is not expected from the present orthodoxy of kinetic analysis, seems to be due to both the deviation of the apparent reaction condition from the idealized measuring conditions and the changes in the reaction process with the sample and measuring conditions. The gradients in the temperature and gaseous pressure and these continuous changes during the course of reaction are

Table 4 The mathematical form of X in eqns. (10) and (11) for the respective method of kinetic calculation.

Method	X^*
Isothermal methods	$\frac{(d\alpha/dt)_H}{(d\alpha/dt)_L}$
Non-isothermal single run methods	$\frac{(d\alpha/dT)_H}{(d\alpha/dT)_L}\frac{f(\alpha_L)}{f(\alpha_H)}$
Non-isothermal isoconversion methods	$\frac{(d\alpha/dT)_H}{(d\alpha/dT)_L}\frac{\beta_H}{\beta_L}$
Non-isothermal peak methods	$\frac{f'(\alpha_L)}{f'(\alpha_H)}\frac{T_L^2}{T_H^2}\frac{\beta_H}{\beta_L}$

* β is the heating rate and the subscripts H and L indicate the highest and lowest values, respectively.

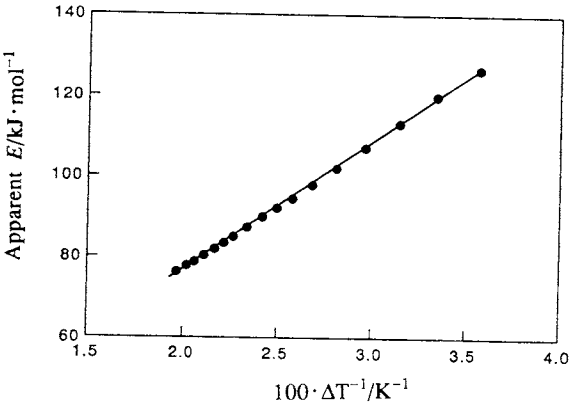

Fig.6 The $1/\Delta T$ dependence of the apparent E values obtained at different α for the non-isothermal dehydration of single crystalline $Li_2SO_4 \cdot H_2O$.

likely to be the important causes of the former[21)-23)]. In this sense, the Controlled Transformation rate Thermal Analysis (CRTA)[24)] has a merit, because the self-generated condition remains constant during the reaction, at least, compared with the traditional isothermal and non-isothermal measurements[25)-27)]. The latter is the case where the apparent Arrhenius parameters are related to several elementary processes[28)], *i.e.*, nucleation, interface chemical reaction and diffusion, which became particularly important in the analysis of the crystallization processes such as molten polymer[29),30)] and quenched glasses[31)-33)]. Any gradual change in the reaction mechanism and/or the rate limiting step during the reaction is also responsible for the change in the kinetic parameters with α[34)-36)].

The Kinetic Analysis

The correlation of the kinetic parameters with the apparent kinetic models does not allow to perform correctly the kinetic analysis using only one experimental TA curve. This problem can be solved, however, if the true activation energy is known. Then the most probable kinetic model can be determined and subsequently the preexponential term is calculated. The method of kinetic analysis is described in the following sections.

Calculation of the Activation Energy

The calculation of activation energy is based on multiple scan methods where several measurements at different heating rates are required, *i.e.*, the isoconversion methods[37)]. Logically the isoconversion methods can be divided into the Ozawa-Flynn-Wall method[38),39)], the Kissinger-Akahira-Sunose method[40)] and the expanded Friedman method[41),42)]. These methods allow to check the invariance of E with respect to α which is one of the basic assumptions in the kinetic analysis[43)].

Among others, the expanded Friedman method has the wider applicability[42)]. Taking logarithms of eqn.(1)

$$\ln\frac{d\alpha}{dt} = \ln[Af(\alpha)] - \frac{E}{RT} \tag{12}$$

The slope of $\ln(d\alpha/dt)$ vs. $1/T$ for a given value of α gives the activation energy. The applicability of eqn.(12) can be estimated by introducing the generalized time θ[44)]:

$$\theta = \int_0^t \exp\left(-\frac{E}{RT}\right)dt \tag{13}$$

First differentiation gives

$$\frac{d\theta}{dt} = \exp\left(-\frac{E}{RT}\right) \tag{14}$$

Combining eqn.(1) with eqn.(14),

$$\frac{d\alpha}{d\theta} = Af(\alpha) \tag{15}$$

Eqn.(1) is thus expressed by

$$\frac{d\alpha}{dt} = \frac{d\alpha}{d\theta}\frac{d\theta}{dt} \tag{16}$$

Eqns. (14) and (16) show that $d\alpha/dt$ is proportional to $\exp(-E/RT)$ at a given α, having the propotional constant of $d\alpha/d\theta$. Since eqns.(14), (15) and (16) hold for any temperature change, eqn.(12) can be applied to any TA data obtained under any condition of temperature change[42)]. Thus eqn.(12) can successfully be used for the TA curves even if the programmed temperature condition was distorted by the self-cooling and/or self-heating as well as for the CRTA curves[45)].

Determination of the Kinetic Model

Once the activation energy has been determined we can find the kinetic model which best describes a measured set of TA data. Malek[7] has shown that for this purpose it is useful to define two special functions $y(\alpha)$ and $z(\alpha)$ which can easily be obtained by simple transformation of experimental data.

Through rearrangement of eqn.(1), the function $y(\alpha)$ is defined as [46]:

$$y(\alpha)=\frac{d\alpha}{dt}\exp(\frac{E}{RT})=Af(\alpha) \qquad (17)$$

The $y(\alpha)$ function corresponds to $d\alpha/d\theta$ and is proportional to the $f(\alpha)$ function. Thus by plotting $y(\alpha)$ dependence, normalized within <0,1> interval, the shape of function $f(\alpha)$ is obtained. The $y(\alpha)$ function is, therefore, characteristic for a given kinetic model $f(\alpha)$ and it can be used as a diagnostic tool for the kinetic model determination. The mathematical condition for the maximum of the $y(\alpha)$ function can be written as:

$$f'(\alpha)=-\frac{df(\alpha)}{d\alpha}=0 \qquad (18)$$

Comparing eqn.(18) with the different form of the respective $f(\alpha)$ (see Table 1), the D_1, D_2, D_3, D_4 and R_n models have a maximum at α_M=0. On the other hand, the *JMA(M)* and *SB(m,n)* models have a maximum at $0<\alpha_M<\alpha_p$. For the *JMA(M)* model, the relationship between the α_M value and kinetic exponent M is represented as:

$$\alpha_M=1-\exp\left(\frac{1-M}{M}\right) \qquad (19)$$

It is written for the *SB(m,n)* model as:

$$\alpha_M=\frac{m}{m+n} \qquad (20)$$

Figure 7 shows schematically the character of the $y(\alpha)$ function with respect to various kinetic model functions. It should be stressed that the shape of the $y(\alpha)$ function is strongly affected by E. Hence the true activation energy is decisive for a reliable determination of the kinetic model because of the correlation of kinetic parameters.

Similarly, we can discuss the mathematical

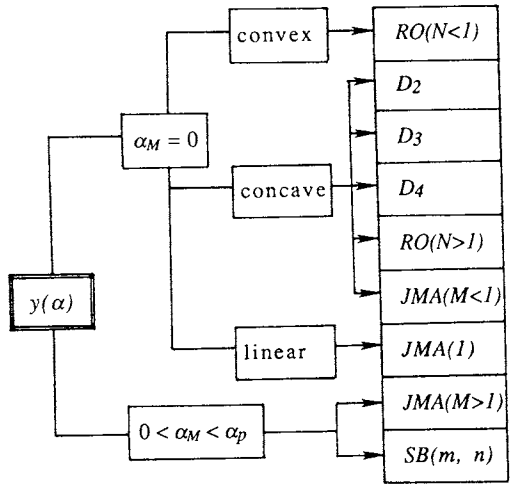

Fig.7 Schematic diagram of the kinetic model determination by using the $y(\alpha)$ function.

properties of the $z(\alpha)$ function. If the temperature rises at a constant rate β, integration of eqn.(1) gives:

$$g(\alpha)=\int_0^\alpha\frac{d\alpha}{f(\alpha)}=\frac{AE}{\beta R}\exp(-x)\left[\frac{\pi(x)}{x}\right] \qquad (21)$$

By combining eqns.(1) and (21), an alternative kinetic equation is obtained:

$$\frac{d\alpha}{dt}=\left[\frac{\beta}{T\pi(x)}\right]f(\alpha)g(\alpha) \qquad (22)$$

After rearrangement of eqn.(22), the $z(\alpha)$ function is defined as[47]:

$$z(\alpha)=\pi(x)\frac{d\alpha}{dt}\frac{T}{\beta}=f(\alpha)g(\alpha) \qquad (23)$$

Differentiation of eqn.(23) with respect to α gives:

$$z'(\alpha)=f'(\alpha)g(\alpha)+1 \qquad (24)$$

In addition, by differentiating eqn.(22)[48]:

$$\left(\frac{d^2\alpha}{dt^2}\right)=\left[\frac{\beta}{T\pi(x)}\right]^2 f(\alpha)g(\alpha)[f'(\alpha)g(\alpha)+x\pi(x)] \qquad (25)$$

By setting eqn.(25) equal to zero, the mathematical condition for the maximum of TA peak is obtained:

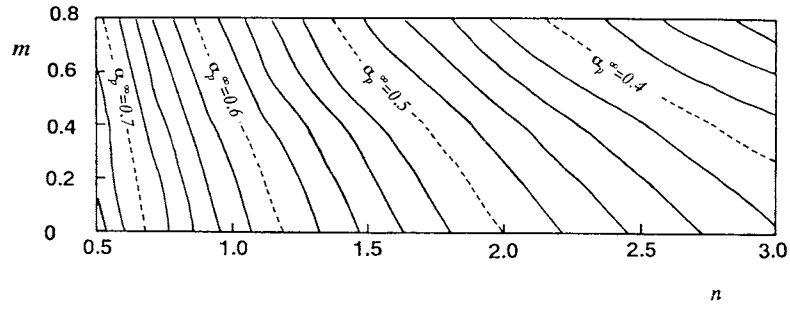

Fig.8 The dependence of the maximum of the $z(\alpha)$ function α_p^∞ on the kinetic exponents for the $SB(m,n)$ kinetic model.

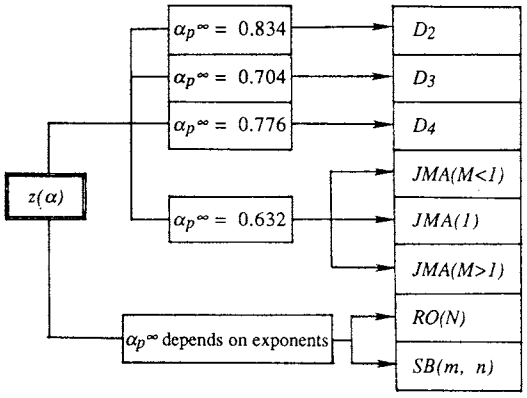

Fig.9 Schematic diagram of the kinetic model determination by using the $z(\alpha)$ function.

$$-f'(\alpha_p)\,g(\alpha_p) = x_p\pi(x_p) \tag{26}$$

When x_p is infinite, eqn.(26) is written as:

$$-f'(\alpha_p^\infty)\,g(\alpha_p^\infty) = \lim_{x_p\to\infty}[x_p\pi(x_p)] = 1 \tag{27}$$

where α_p^∞ is the α_p at $x_p\to\infty$. Comparing eqn.(24) with eqn.(27), it is apparent that at the maximum of the $z(\alpha)$ function eqn.(24) sets equal to zero being fulfilled by α_p^∞. The $z(\alpha)$ function has a maximum at α_p^∞ for all kinetic models summarized in Table 1, having the characteristic value of α_p^∞ [7] for respective kinetic models. It is interesting that the α_p^∞ value practically does not depend on the value of activation energy used to calculate $z(\alpha)$ (in fact it varies within 1% of the theoretical value). An important fact is that the α_p^∞ is invariant with respect to the kinetic exponent for the *JMA(M)* model. On the other hand for both the *RO(N)* and *SB(m,n)* models the parameter α_p^∞ depends on the values of kinetic exponents as shown in Fig. 8. Figure 9 shows schematically the property of $z(\alpha)$ function for the respective kinetic model function.

It is evident that the shape of the $y(\alpha)$ function as well as the maximum α_p^∞ of the $z(\alpha)$ function can be used as a guide to select the kinetic model. Table 5 summarizes the property of $y(\alpha)$ and the value of α_p^∞ for the respective $f(\alpha)$. Both α_M and α_p^∞ parameters are especially useful in this respect. Their combination allows the determination of the most suitable kinetic model as shown by the scheme in Figs. 7 and 9. As we can see, the empirical *SB(m,n)* model gives the best description of TA data if $\alpha_p^\infty \neq 0.632$ and $\alpha_M \in (0,\alpha_p)$. According to our experience these conditions are fulfilled for some solid-state processes[49),50)].

Calculation of Kinetic Exponents

Once the kinetic model is determined the kinetic exponents can be calculated for *RO(N)*, *JMA(M)* or *SB(m,n)* model. The calculation method depends on the kinetic model and is described below.

***RO(N)* model:** The kinetic exponent $N\neq 0$ for this model can be calculated iteratively using the equation:

$$\alpha_p = 1 - \left[1 + \frac{1-N}{N} x_p\pi(x_p)\right]^{1/(N-1)} \tag{28}$$

This equation is obtained from eqn.(26) and was derived originally by Gorbachev[51)] for a simplified approximation: $\pi(x_p)=1/(x_p+2)$

***JMA(M)* model:** If the $y(\alpha)$ function has a maximum

Table 5 The property of the $y(\alpha)$ function and the value of α_p^{∞} for the respective kinetic model function.

Model	$y(\alpha)$	α_p^{∞}
JMA(M)	$M<1$; concave	0.632
	$M=1$; linear	0.632
	$M>1$; maximum	0.632
R_2	convex	0.750
R_3	convex	0.704
D_2	concave	0.834
D_3	concave	0.704
D_4	concave	0.776

at $\alpha_M \in (0,\alpha_p)$, *i.e.* for $M>1$, then the kinetic exponent M is calculated using the eqn.(19):

$$M = \frac{1}{1+\ln(1-\alpha_M)} \tag{29}$$

***SB(m,n)* model:** Rearrangement of eqn.(20) gives the ratio of kinetic exponents $p=m/n$:

$$P = \frac{\alpha_M}{1-\alpha_M} \tag{30}$$

From the relationship of eqn.(17):

$$\ln y(\alpha) = \ln A + n\ln[\alpha^P(1-\alpha)] \tag{31}$$

The kinetic parameter n corresponds to the slope of linear dependence of ln $y(\alpha)$ versus $\ln[\alpha^P(1-\alpha)]$ for $\alpha \in (0.2, 0.8)$. Then the second kinetic exponent is $m=pn$.

Calculation of the Preexponential Factor

Knowing the value of activation energy and the kinetic model the preexponential factor is calculated. On determining the preexponential factor, it should be considered that the constant value of A at different values of α is also the prerequisite for the application of eqn.(1), as is the case of E. Rearrangement of eqn.(17) gives:

$$A = \frac{y(\alpha)}{f(\alpha)} \tag{32}$$

According to eqn.(32), the value of A at different α can be calculated allowing to check the invariance of A with respect to α.

Alternatively, using the condition of maximum of a TA peak, the preexponential factor is calculated by the following equation[7),49)]:

$$A = -\frac{\beta x_p}{Tf'(\alpha_p)} \exp(x_p) \tag{33}$$

Software for Kinetic Analysis

If is rather surprising that the distortion of the kinetic parameters by the apparent kinetic model as well as the mutual correlation of the Arrhenius parameters are very often ignored even in the commercially available kinetic software. The experimentally resolved shape of TA curves does not always provide the satisfactory source of kinetic data, because the preliminary requisite of the kinetic equation is not guaranteed during the TA measurement. Although the precise measurement of temperature is always required for a better thermal analysis, the reliability of the TA data is influenced by the nature of reaction under investigation and the sample and measuring conditions are selected depending on the purpose of the kinetic study. Changes in the kinetic parameters for the empirically same reaction may be a simple consequence of trying to describe a complex process by computing the Arrhenius parameters, accepting changes of many order of magnitude of practical reaction condition without question or test[52)]. In this respect, the kinetic software must include the check system of the reliability of the TA curves as a possible kinetic

source. The simple example is the examination of the practical heating rate during the course of reaction, because the programmed heating or cooling rate is distorted by the self-cooling and/or self-heating of the reaction[22),31)].

The method of kinetic calculation has to be selected based on the above test of the TA data in the light of the limitation of the kinetic method. Comparison of the kinetic parameters determined using various methods of kinetic calculation provides us with less information on the significance of the kinetic parameters determined. The invariance of the apparent value of E is a measure of the constancy of the reaction mechanism among various runs at different heating rates. Mathematically, the further kinetic analysis is possible only on the basis of the constant, thus characteristic, value of E. In a practical sense, the fluctuation of the value of E diminishes the suitability of the kinetic analysis and regulates the quality of kinetic analysis, *i.e.*, whether it is really physico-chemical or empirical. The acquisition of the most relevant kinetic information from the experimentally resolved TA curves should only be possible on the appropriate level of kinetic analysis[47)].

Taking account of the above discussion, the kinetic software is required to have both the mathematically and practically oriented algorithm including the check system of the kinetic analysis. The checking process itself has a kinetic significance and also serves for the evaluation of meaningful kinetic parameters. Any method of the kinetic calculation cannot accommodate the widely distributed conditions which depend on the type of TA instrument, the nature of reaction processes and the experimental factors.

Conclusion

It was shown that the kinetic exponent in the kinetic model function, the activation energy and the preexponential factor are mutually correlated. As a consequence of this correlation any TA curve can be described by an apparent kinetic model instead of the appropriate one with a certain value of apparent Arrhenius parameters. The use of the conventional kinetic model is sometimes to be a source of the distortion of the Arrhenius parameters, because the real heterogeneous process detected by TA measurements is hardly to be described by the conventional kinetic model function which is derived based on the geometrically well defined bodies under strictly isothermal condition. The empirical kinetic model, $SB(m,n)$, accommodates the discrepancy of the real process from the idealized process, with the flexibility enough to describe the real process as closely as possible. In terms of the accommodation function $a(\alpha)$, the physico-geometry of the process could also be predicted from the empirical kinetic exponents with non-integral values. Mutual dependence of the Arrhenius parameters results also from the change in the temperature interval of kinetic analysis. This is due to the poorly controlled reaction condition including the self-generated condition. In this respect, the CRTA has a merit, because the self-generated condition remains constant during the reaction, at least, compared with the traditional isothermal and non-isothermal measurements.

Therefore, the kinetic analysis of TA data cannot be successful unless the true value of the activation energy is known. The isoconversion method of calculating the activation energy is useful allowing to check the invariance of the activation energy during the course of reaction. For such TA curves providing the constant and characteristic value of E, the functional relationships $y(\alpha)$ and $z(\alpha)$ are very useful in elucidating the kinetic model function. These functions allow to check the applicability of the conventional physico-geometry based kinetic models and to extend the kinetic understanding based on the more sophisticated kinetic models.

ACKNOWLEDGMENT

The authors wish to thank Dr. T. Ozawa for reading the manuscript and for helpful suggestions.

References

1) J. Sestak(ed.), Reaction Kinetics by Thermal Analysis, *Thermochim. Acta (Special issue)* **203**, 1992.

2) J. Sestak, *J. Therm. Anal.* **16**, 503 (1979); **33**,

1263 (1988).
3) J. Sestak, Thermophysical Properties of Solids, Their Measurements and Theoretical Thermal Analysis, Elsevier, Amsterdam (1984).
4) J. Sestak, *J. Therm. Anal.* **36**, 1977 (1990).
5) N. Koga, J. Sestak and J. Malek, *Thermochim, Acta* **188**, 333 (1991).
6) J. Malek and J. M. Criado, *Thermochim, Acta* **203**, 25 (1992).
7) J. Malek, *Thermochim. Acta* **200**, 257 (1992).
8) E. S. Freeman and B. Carroll, *J. Phys. Chem.* **62**, 394 (1958).
9) N. Koga and H. Tanaka, *J. Therm Anal*, in press.
10) R. Ozao and M. Ochiai, *J. Ceram. Soc. Jpn.* **101**, 263 (1993).
11) J. Sestak in D. Dollimore (ed.), Thermal Analysis, Proc. 2nd ESTAC in Aberdeen, J. Wiley, London (1981), p. 115.
12) T. Kemeny and J. Sestak, *Thermochim. Acta* **110**, 113 (1987).
13) J. Sestak and G. Berggern, *Thermochim. Acta* **3**, 1 (1971).
14) V. M. Gorbatchev, *J. Therm. Anal.* **18**, 194 (1980).
15) N. Koga and J. Sestak, *Thermochim. Acta* **182**, 201 (1991).
16) J. Sestak in H. G. Wiedeman (ed.), Thermal Analysis, Proc. 6th ICTA, Birkhauser, Stuttgart, Vol. 1 (1980), p. 29.
17) J. Sestak, *J. Therm. Anal.* **33**, 1263 (1988).
18) N. Koga and J. Sestak, *J. Therm. Anal.* **37**, 1103 (1991).
19) N. Koga and H. Tanaka, *J. Therm. Anal.* **37**, 347 (1991).
20) J. Flynn, *J. Therm. Anal.* **36**, 1269 (1990).
21) J. Sestak, *Talanta* **13**, 567 (1966).
22) H. Tanaka and N. Koga, *J. Therm. Anal,* **36**, 2601 (1990).
23) N. Koga and H. Tanaka, *Thermochim. Acta* **183**, 125 (1991).
24) J. Rouquerol, *J. Therm. Anal.* **5**, 203 (1973).
25) H. Tanaka, *Netsu Sokutei* **19**, 32 (1992). (in Japanese)
26) J. Malek, J. Sestak, F. Rouquerol, J. Rouquerol, J. M. Criado and A. Ortega, *J. Therm. Anal.* **38**, 71 (1992).
27) J. P. Czarnecki, N. Koga, V. Sestakova and J. Sestak, *J. Therm. Anal.* **38**, 575 (1992).
28) J. Sestak, *Phys. Chem. Glasses* **15**, 137 (1974).
29) T. Ozawa, *Polymer* **12**, 150 (1971).
30) T. Ozawa, *Bull. Chem. Soc. Jpn.* **57**, 639 (1984); 952 (1984).
31) J. Sestak, *Thermochim. Acta* **98**, 339 (1986).
32) N. Koga, J. Sestak and Z. Strnad, *Thermochim. Acta* **203**, 361 (1992).
33) N. Koga and J. Sestak, *Bol. Soc. Esp. Ceram. Vidr.* **31**, 185 (1992).
34) H. Tanaka and N. Koga, *J. Phys. Chem.* **92**, 7023 (1988).
35) N. Koga and H. Tanaka, *J. Phys. Chem.* **93**, 7793 (1989).
36) N. Koga and H. Tanaka, *Solid State Ion.* **44**, 1 (1990).
37) T, Ozawa, *Thermochim. Acta* **203**, 159 (1992).
38) T. Ozawa, *Bull. Chem, Soc. Jpn.* **38**, 1881 (1965).
39) T. Ozawa, *J. Therm. Anal.* **2**, 301 (1970).
40) H. E. Kissinger, *Anal. Chem.* **29**, 1702 (1957).
41) H. L. Friedman, *J. Polym. Sci., Part C* **6**, 183 (1964).
42) T. Ozawa, *J. Therm. Anal.* **31**, 547 (1986).
43) T. Ozawa, *Netsu Sokutei* **1**, 2 (1974). (in Japanese)
44) T. Ozawa, *Thermochim. Acta* **100**, 109 (1986).
45) N. Koga and H. Tanaka, *Thermochim. Acta*, in press.
46) J. M. Criado, J. Malek and A. Ortega, *Thermochim. Acta* **147**, 377 (1989).
47) J. Malek, *Thermochim. Acta* **138**, 337 (1989).
48) J. Malek and J. M. Criado, *Thermochim. Acta* **164**, 199 (1990).
49) J. Malek and V. Smrcka, *Thermochim. Acta* **186**, 153 (1991).
50) J. Malek, *J. Non-Cryst. Solids* **107**, 323 (1989).
51) V. M. Gorbachev, *J. Therm. Anal.* **27**, 151 (1983).
52) P. D. Garn, *Thermochim, Acta* **135**, 71 (1988).

要　旨

非等温的速度論におけるデータ処理と

Data Treatment in Non-isothermal Kinetics and Diagnostic Limits of Phenomenological Models

現象学的モデルの判別限界

固相反応の動力学的モデルは，厳密な等温的条件下での幾何学的に理想化された固体反応物に対する形式的な記述をもとにして導かれる。これらの仮定は，実際のプロセスに適合しない場合が多い。実際のプロセスと理想化された動力学的モデルとの差異は，得られる動力学的パラメータの真の値からの偏差としてあらわれる。この観点から，実際のプロセスをできるだけ正確に記述する経験的関数を用いることが有用である。この場合，不均一反応速度論のモデル関数は，より単純な均一反応速度論におけるモデル関数の歪曲したものであると考えられ，数学的には収容関数を掛け合わせることにより導くことができる。この経験的なモデル関数は，非等温的プロセスの等温的プロセスとの違いを収容するものとも考えられる。経験的に観察されるアレニウスパラメータの相互依存性は，熱分析における測定条件の制御に関する問題点と不適切な動力学的データ処理から生じることが多く，数学的にはアレニウスの関係式において速度定数が指数型で表されることと関係している。等変化率法では，ある反応のプロセス全体を通して活性化エネルギーが一定であることを確認することができ，以後の動力学的データ処理の指針となる。一定の活性化エネルギーが得られるプロセスに対しては，従来の速度式から導かれる二つの関数依存性を用いて動力学的モデル関数を決定することができる。

Thermochimica Acta xxx (2011) xxx–xxx

Contents lists available at ScienceDirect

Thermochimica Acta

journal homepage: www.elsevier.com/locate/tca

Short communication

Fourty years of the Šesták–Berggren equation

Peter Šimon*

Institute of Physical Chemistry and Chemical Physics, Faculty of Chemical and Food Technology, Slovak University of Technology, Radlinského 9, SK-812 37, Bratislava, Slovak Republic

ARTICLE INFO

Article history:
Received 20 February 2011
Received in revised form 14 March 2011
Accepted 23 March 2011
Available online xxx

Keywords:
Šesták–Berggren equation
Single-step approximation
Model-fitting method
Mechanistic interpretation

ABSTRACT

The Šesták–Berggren equation, representing a powerful tool for the description of kinetic data by the model-fitting methods, is analyzed. It is discussed that the exponents in the conversion function are non-integer in general and that the conversion function may not have a mechanistic interpretation. Within the framework of single-step approximation, the Šesták–Berggren equation enables to describe the kinetics of complex condensed-state processes without a deeper insight into their mechanism.

Kinetics of the processes in condensed phase is frequently described by the so-called general rate equation representing the reaction rate $d\alpha/dt$ as a product of two mutually independent functions:

$$\frac{d\alpha}{dt} = k(T)f(\alpha) \quad (1)$$

The temperature function, $k(T)$, depends solely on temperature T and the conversion function, $f(\alpha)$, depends only on the conversion of the process, α. The temperature function is prevailingly interpreted as the rate constant and the conversion function is believed to reflect the mechanism of the process.

Fourty years ago, a paper by Šesták and Berggren [1] appeared in this journal introducing in Eq. (1) a three-parameter conversion function for a generalized description of reaction kinetics. The equation is often named after their authors, i.e. the Šesták–Berggren equation (habitually abbreviated as the SB equation):

$$\frac{d\alpha}{dt} = k(T)\alpha^m(1-\alpha)^n[-] \quad (2)$$

where m, n, and p are the (generally non-integer) exponents. Later on, Gorbachev [2] demonstrated that, for isothermal conditions, Eq. (2) can be transformed into three invariant expressions with two exponents only. Among them, the following form is the one which is most frequently employed:

$$\frac{d\alpha}{dt} = k(T)\alpha^a(1-\alpha)^b \quad (3)$$

The exponents a and b in Eq. (3) may differ from those m and n introduced in Eq. (2).

Eq. (3) can be encountered in the literature published before 1971. Erofeev and Mitskevich in 1961 [3] pointed out that the expansion and rearrangement of the differentiated form of the Yerofeev equation lead to Eq. (3). As early as in 1940, Akulov reported Eq. (3) where the constants a and b called the "constants of homogeneity" [4]. Eq. (3) is also quite frequently cited in the literature as an extended form of the Prout and Tompkins autocatalytic equation [5], for example in [6–9]. Nonetheless, Eq. (3) is generally considered a transformation of Eq. (2) so that it is equally called the SB equation.

Eq. (3) is widely applied to the study of not only isothermal, but also non-isothermal processes; mathematical correctness of either description was justified in [10]. Later it was shown [11] that this two-parameter model retains its physical meaning only for $a \leq 1$. Málek pointed out that the classical nucleation-growth equation (often abbreviated as JMAYK) is actually a special case of this two-parameter SB model and thus SB equation represents a plausible alternative description for the crystallization processes taking place in non-crystalline solids [12]. The increasing value of the exponent a indicates a more important role of the precipitated phase on the overall kinetics. It also appears that a higher value of the second exponent ($b > 1$) indicates increasing reaction complexity; however, the temptation to relate the values of a and b to a reaction mechanism can be doubtful and should be avoided [12] without complementary measurements [13,14].

Due to its ability to describe variety of kinetic data both of organic and inorganic origin [9], the SB equation attracts much attention. It was believed that it can be considered a universal expression for kinetic models [15]. For certain combinations

* Tel.: +421 2 59325530; fax: +421 2 52926032.
E-mail address: peter.simon@stuba.sk

0040-6031/$ – see front matter © 2011 Elsevier B.V. All rights reserved.
doi:10.1016/j.tca.2011.03.030

of exponents, the conversion function in SB equation can merge in most conversion functions representing mechanisms of processes. For further improvement of the mechanistic interpretation, multiplying the SB equation by an accommodation constant was suggested [16]. Nevertheless, it was recognized that kinetic models of solid-state reactions are often based on a formal description of geometrically well-defined bodies under isothermal conditions; for real processes, these assumptions are evidently incorrect [17].

In contrast with the mechanistic interpretations of Eq. (1) mentioned above, there is the idea of the single-step approximation [18,19]. The history and contradictions of the concept of single-step reaction have been discussed in [20]. The approximation is based on the fact that the processes in condensed phase tend to occur in multiple steps that have different rates. Each reaction step should be described by its own kinetic equation. It has been demonstrated that, neither for the simplest cases, the kinetic equations characterizing complex mechanisms cannot be reduced into the factorized form of Eq. (1) [21]. Hence, it has been concluded that Eq. (1) is not a true kinetic equation; it is just a mathematical tool for the description of kinetic data [18,19,21]. The single-step approximation resides in replacing the set of differential rate equations by the single-step generalized rate equation. The functions $k(T)$ and $f(\alpha)$ represent, in general, just the temperature and conversion components of the kinetic hypersurface; this hypersurface is a dependence of conversion as a function of time and temperature [18]. Thus, the temperature function may not be the rate constant and the conversion function may not reflect the reaction mechanism.

The value and wide applicability of the SB equation surpasses in the light of the single-step approximation. The conversion functions in Eqs. (2) or (3) are able to describe both the S-shaped accelerating kinetic curves and the n-th order ones. Due to the possibility of adjustment of the exponents, the function is very versatile and flexible. In general, the values of exponents may not reflect the reaction mechanism; on the other hand, they enable to describe kinetic data and modeling the kinetics of the overall process without a deeper insight into its mechanism. The SB equation provides purely formal description of the kinetics and it should be applied and understood in this way.

The Šesták–Berggren equation represents a powerful tool for the description of kinetic data by the model-fitting methods. According to SCOPUS, the paper [1] was cited 316 times since 1996. Since 1971, the paper was cited nearly 600 times and probably is the most cited paper in the history of almost twenty two thousand papers published in Thermochimica Acta. There are no doubts that the SB equation will continue being widely applied also in future, either in the form of Eq. (2) or Eq. (3).

Acknowledgements

The author would like to express his cordial thanks to Dr. S. Vyazovkin for invaluable comments and for providing the old Russian literature sources.

The financial support from the Slovak Scientific Grant Agency, grant No. VEGA 1/0660/09, is gratefully acknowledged.

References

[1] J. Šesták, G. Berggren, Study of the kinetics of the mechanism of solid-state reactions at increasing temperature, Thermochim. Acta 3 (1971) 1–12.
[2] V.M. Gorbachev, Some aspects of Šesták's generalized kinetic equation in thermal analysis, J. Therm. Anal. 18 (1980) 193–197.
[3] D.A. Young, Decomposition of Solids, Pergamon Press, Oxford, 1966, p. 35.
[4] E.A. Prodan, Inorganic Topochemistry, Nauka i Technika, Minsk, 1986, p.153 (in Russian).
[5] E.G. Prout, F.C. Tompkins, The thermal decomposition of potassium permanganate, Trans. Faraday Soc. 40 (1944) 488–498.
[6] J. Šesták, Review of kinetic data evaluation from nonisothermal and isothermal TG data, Silikáty 11 (1967) 153 (in Czech).
[7] W.L. Ng, Thermal decomposition in the solid state, Aust. J. Chem. 28 (1975) 1169–1178.
[8] J. Malek, T. Mitsuhashi, J.M. Criado, Kinetic analysis of solid-state processes, J. Mater. Res. 16 (2001) 1862–1871.
[9] A.K. Burnham, Application of the Šesták–Berggren equation to organic and inorganic materials of practical interest, J. Therm. Anal. Calorim. 60 (2000) 895–908.
[10] T. Kemény, J. Šesták, Comparison of crystallization kinetics determined by isothermal and non-isothermal methods, Thermochim. Acta 110 (1987) 113–129.
[11] J. Málek, J.M. Criado, J. Šesták, J. Militký, The boundary conditions for kinetic models, Thermochim. Acta 153 (1989) 429–432.
[12] J. Málek, Kinetic analysis of crystallization processes in amorphous materials, Thermochim. Acta 355 (2000) 239–253.
[13] J. Šesták, Thermophysical Properties of Solids: A Theoretical Thermal Analysis, Elsevier, Amsterdam, 1984.
[14] J. Šesták, Science of heat and thermophysical studies: a generalized approach to thermal analysis, Elsevier, Amsterdam 2005.
[15] J. Málek, J.M. Criado, Is the Šesták–Berggren equation a general expression of kinetic models? Thermochim. Acta 175 (1991) 305–309.
[16] L.A. Pérez-Maqueda, J.M. Criado, P.E. Sánchez-Jiménez, Advantages of combined kinetic analysis of experimental data obtained under any heating profile, J. Phys. Chem. A110 (2006) 12456–12462.
[17] N. Koga, J. Malek, J. Sestak, H. Tanaka, Data treatment in non-isothermal kinetics and diagnostic limits of phenomenological models, Netsu Sokutei 20 (1993) 210–223.
[18] P. Šimon, Single-step kinetics approximation employing non-Arrhenius temperature functions, J. Therm. Anal. Calorim. 79 (2005) 703–708.
[19] P. Šimon, Considerations on the single-step kinetics approximation, J. Therm. Anal. Calorim. 82 (2005) 651–657.
[20] S. Vyazovkin, Kinetic concepts of thermally stimulated reactions in solids: a view from a historical perspective, Int. Rev. Phys. Chem. 19 (2000) 45–60.
[21] P. Šimon, The single-step approximation: attributes, strong and weak sides, J. Therm. Anal. Calorim. 88 (2007) 709–715.

preferentially etched out during the thinning process before examination.

C. Phaal
G. S. Woods

Adamant Research Laboratory,
Crown Mines, Johannesburg,
South Africa.

[1] Meyer, H. O. A., and Milledge, H. J., *Nature*, **199**, 167 (1963).
[2] Lonsdale, K., and Milledge, H. J., *Physical Properties of Diamond* (edit. by Berman, R.), 12 (Clarendon Press, Oxford, 1965).
[3] Phaal, C., and Zuidema, G., *Phil. Mag.*, **14**, 79 (1966).
[4] Lonsdale, K., Milledge, H. J., and Nave, E., *Min. Mag.*, **32**, 185 (1959).
[5] Pearson, W. B., *A Handbook of Lattice Spacings and Structures of Metals and Alloys*, 500 (Pergamon Press, London, 1958).

CHEMISTRY

Determination of Activation Energies of Chemical Reactions by Differential Thermal Analysis

A number of articles have been published dealing with the differential thermal analysis (DTA) of chemical reaction kinetics[1–5]. Only one of these, however, gives a direct method for determining the activation energy (E) of the chemical reaction[4]. In this method, DTA curves are recorded at several different rates of heating. The results are then plotted as $\ln b/T_m^2$ against $1/T_m$, where T_m is the peak temperature in ° K (the temperature of point B, Fig. 1), and b is the rate of heating. The magnitude of E is calculated from the angle between this straight line and the abscissa. This procedure has two principal shortcomings: (1) it is necessary to record several DTA curves with various rates of heating; and (2) it is necessary to use a special programming device to control the temperature. This device must be capable of providing linear heating at a number of rates of heating. The latter condition imposes serious technical difficulties, because all the DTA apparatuses at present available are adjusted for only one rate of heating.

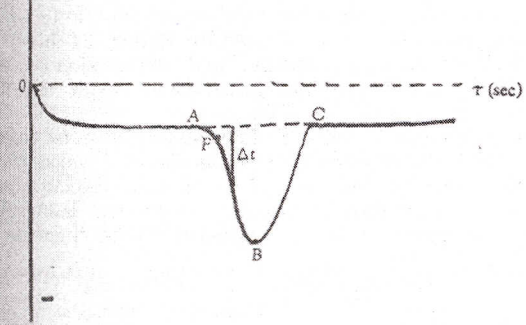

Fig. 1. Formalized differential thermal curve, showing the various attributes of the thermal effect. For explanation see text.

The present communication puts forward a method for determining E from a single DTA curve recorded at an arbitrary rate of heating.

Let us consider this method applied to the decomposition reactions of solids. The given substance dissociates over a particular range of temperature and gives rise to the thermal effect ABC on the DTA curve (Fig. 1). It is well known[2,6] that the deviation from the baseline (Fig. 1) in the initial stages of the reaction is satisfactorily described by

$$\Delta t = S\frac{d\alpha}{d\tau} \qquad (1)$$

where Δt is the deviation from baseline (° C); S is the area of the thermal effect (° C × sec); $d\alpha/d\tau$ is the rate of the reaction; and α is the extent of the reaction.

The rate of a chemical reaction is usually described by

$$\frac{d\alpha}{d\tau} = A_0 f(\alpha) \exp(-E/RT) \qquad (2)$$

where A_0 is a constant, $f(\alpha)$ is a function of the extent of reaction (it is often assumed that $f(\alpha) = (1-\alpha)^n$, where n is the order of reaction; but in more general cases $f(\alpha) = \alpha^m(1-\alpha)^n$, where m and n are the constants).

Substituting equation (1) into equation (2), and taking logarithms, the following equation can be obtained

$$\ln \Delta t = C - \ln f(\alpha) - \frac{E}{RT} \qquad (3)$$

where C is a constant which combines all the constants of equations (1) and (2), and T is the temperature in ° K corresponding to a given value of Δt.

Under normal isothermal conditions, the only variable determining the reaction rate is α. In DTA, however, the temperature also varies. It can easily be shown that when the value of α lies between 0·05 and 0·8 (approximately up to the peak of the thermal effect) at the usual heating rates the change in temperature has a greater effect on Δt than the change in α at the normal rates of heating (10°–40° C/min). To an approximation, therefore, the term $\ln f(\alpha)$ can be neglected and equation (3) written in the following form*

$$\ln \Delta t = C^1 - \frac{E}{RT} \qquad (4)$$

The values of Δt are taken directly from the DTA curve in units of length (cm or mm) as is shown in Fig. 1.

Table 1. Activation Energies for Some Reactions

Substance	Type of reaction	E (experimental)	E (from the literature)	Ref.
$CuSO_4\,5H_2O$	Dehydration	17·9	18·0	7
$CaCO_3$	Dissociation	35·4	35–48	7
$MgCO_3$	,,	32·0	32·4	5
$CaC_2O_4{\cdot}H_2O$	Dehydration	21·0	20–22	8

The errors of these determinations are estimated at between 15 and 20 per cent.

The interval measured is approximately represented by the portion FB of the curve in Fig. 1. The measurements are taken not from the point at which the thermal effect begins (point A, Fig. 1), but at some distance from it (approximately from the point of maximum curvature, F). Table 1 gives values of E determined for the decomposition reactions of various substances.

G. O. Piloyan
I. D. Ryabchikov
O. S. Novikova

Institute of Geology and Exploitation of Combustible Materials,
U.S.S.R. Academy of Sciences,
Moscow.

* Under the conditions indicated, equation (4) also comprises processes obeying the equations of diffusion kinetics.

[1] Borchardt, H. J., and Daniels, F., *J. Amer. Chem. Soc.*, **79**, 41 (1957).
[2] Borchardt, H. J., *J. Inorg. Nucl. Chem.*, **12**, 252 (1960).
[3] Blumberg, A. A., *J. Phys. Chem.*, **63**, 1129 (1959).
[4] Kissinger, H. E., *J. Res. Nat. Bur. Stand.*, **57**, 217 (1956).
[5] Kissinger, H. E. *Anal. Chem.*, **29**, 1702 (1957).
[6] Piloyan, G. O., *Introduction to the Theory of Thermal Analysis*, 134 (Izd. Nauka, in Russian, 1964).
[7] Garner, W., *Chemistry of the Solid State*, 294 in the Russian translation (Moscow, 1961).
[8] Bancroft, G. M., and Gesser, H. D., *J. Inorg. Nucl. Chem.*, **27**, 1537 (1965).

Microwave Rotation Spectra of Ethyl Acetylene and Ethyl Isocyanide

The rotation spectra of ethyl derivatives continue to be of interest for determining structure parameters and the force field of these molecules[1–5]. We have measured the rotation spectra of two further members of this series, ethyl acetylene and ethyl isocyanide.

Solid State Ionics 63–65 (1993) 245–254
North-Holland

SOLID
STATE
IONICS

Diagnostic limits of phenomenological models of heterogeneous reactions and thermal analysis kinetics

Jaroslav Šesták

Division of Solid State Physics, Institute of Physics of the Academy of Sciences of the Czech Republic, Cukrovarnická 10, 162 00 Prague, Czech Republic

and

Jiří Málek

Joint Laboratory of Solid State Chemistry of the Academy of Sciences of the Czech Republic, and University of Chemical Technology, Čs. Legií sq. 565, 532 10 Pardubice, Czech Republic

Kinetic models of solid-state reactions are often based on a formal description of geometrically well defined bodies treated under strictly isothermal conditions; for real processes these prepositions are evidently incorrect. It can be equally useful to find an empirical function containing the smallest possible number of constants. In such a case the models of heterogeneous kinetics can be assumed as a distorted (fractal) case of the simpler homogeneous kinetics and mathematically treated by multiplying by an "accommodation" function. In addition, the conventional thermoanalytical (TA) studies apply intentionally the experimental conditions with constant heating and/or cooling where the model's validity must again be investigated. The general method of kinetic data evaluation is proposed to include two-step evaluation: first, determining the activation energy, E, from a set of TA curves at different heating rates, and second, using the pre-established E to search for the reaction mechanism by analyzing the entire course of the single TA curve. In this respect the possibility of a simultaneous determination of all kinetic data is discussed. The computer method is recommended to be based on the evaluation of two specific functions available for a direct derivation from experimental data.

1. Introduction

In contradiction to the well established spot measurements frequently employed to investigate solid-state reactions, although affected by inadequate freeze-in and poor localization of the reaction, the centered measurements of a property representing the average state of a sample are often considered less convenient due to the superstitiously bad reputation of its mere phenomenological character. The latter group is represented by methods of thermal analysis (TA) carried out under constant heating and/or cooling often treated in terms of a homogeneous-like kinetic description yielding fractal values of reaction orders assumed to have meaningless sense in heterogeneous kinetics. However, even the homogeneous reactions exhibiting non-randomness of the reactant distribution and/or diffusion-controlled subprocess can be described by reactions on fractal domains, the hallmark being the anomalous reaction orders. It is clear that the present state of the art of the thermal analysis kinetics [1] as applied to heterogeneous reactions is not appropriate to the sophisticated means available in solid-state chemistry, the linkage of most treatments to the traditional geometrical description being very firm and hard to overcome [1–3]. The use of phenomenological models has been criticized [2] but a unified approach is still missing as well as a correlation between the microscopic process (detectable only locally under not well guaranteed conditions) and the macroscopic process (capable of measuring in situ even at changing temperatures). Our philosophy is to show that we can merely distinguish proportionable relevancy of the individual groups of phenomenological models to match with the gradual increase

of complexity of an experimentally determined kinetic curve from TA measurements of the reaction investigated.

Extraction of the maximum relevant information from non-isothermal data obtained by such (TA) techniques and a consequent kinetic process modeling are typical tasks of data treatment [1]. The problem of the validity and applicability of mathematical models in kinetic analysis of TA data is still considered a very controversial topic [2]. Apart from the question of the physical meaning of kinetic parameters (which has not been answered until now) there are several problems inherent in the mathematical formalism used for the description of kinetic processes [3]. The aim of this paper is to discuss the possibilities and limitations of kinetic analysis of non-isothermal data.

In the following section we first briefly review the mathematical relationship used to describe TA data. A subsequent section presents some consequences of the mutual correlation of kinetic parameters and their implications for a reliable kinetic analysis. Finally, a completely new way of kinetic analysis is outlined so as to eliminate the effect of experimental conditions. The method allows the determination of the most suitable kinetic model and calculation of a complete set of kinetic parameters.

2. The kinetic equation

Most reactions studied by TA techniques can be described by an equation:

$$d\alpha/dt = A\, e^{-x} f(\alpha)\,, \qquad (1)$$

where $x = E/RT$ is the reduced activation energy. The function $f(\alpha)$ represents a mathematical expression of the kinetic model.

There are several kinetic models derived from the geometry of the reaction interface [3]. The mathematical formulae of the most frequently cited models are summarized in table 1. These kinetic model functions derived on the basis of physical-geometrical assumptions of regularly shaped bodies evidently can hardly describe real heterogeneous systems where we have to consider, for instance, irregular shapes of reacting bodies, polydispersity, shielding and overlapping effects of phases involved in the process, etc.; see fig. 1. From this point of view it would be useful to find an empirical $f(\alpha)$ function containing the smallest possible number of constants, so that it is flexible enough to describe real TA data as closely as possible [3]. Later this concept led to an idea that such an empirical kinetic model would provide a general expression for all kinetic equations shown in table 1.

Unfortunately, these two aspects are very often confused. So we believe it will be useful to discuss these problems, which influence the applicability of the empirical kinetic models in thermal analysis.

3. The empirical kinetic models

Twenty years ago, Šesták and Berggren [4] proposed an empirical kinetic model in the form

$$f(\alpha) = \alpha^m (1-\alpha)^n - \ln(1-\alpha)]^r\,. \qquad (2)$$

It was believed [2,3] that this kinetic equation, containing as many as three exponential terms, is capable of describing any TA curve. Further mathematical analysis [5] of eq. (2) has shown, however, that no more than two kinetic exponents are nec-

Table 1
The kinetic models.

Model	Symbol	$f(\alpha)$
Johnson–Mehl–Avrami	A_n	$n(1-\alpha)[-\ln(1-\alpha)]^{1-1/n}$
2D reaction	R_2	$(1-\alpha)^{1/2}$
3D reaction	R_3	$(1-\alpha)^{1/3}$
2D diffusion	D_2	$1/[-\ln(1-\alpha)]$
Jander equation	D_3	$\frac{3}{2}(1-\alpha)^{2/3}/[1-(1-\alpha)^{2/3}]$
Ginstling–Brounshtein	D_4	$\frac{3}{2}[(1-\alpha)^{-1/3}-1]$

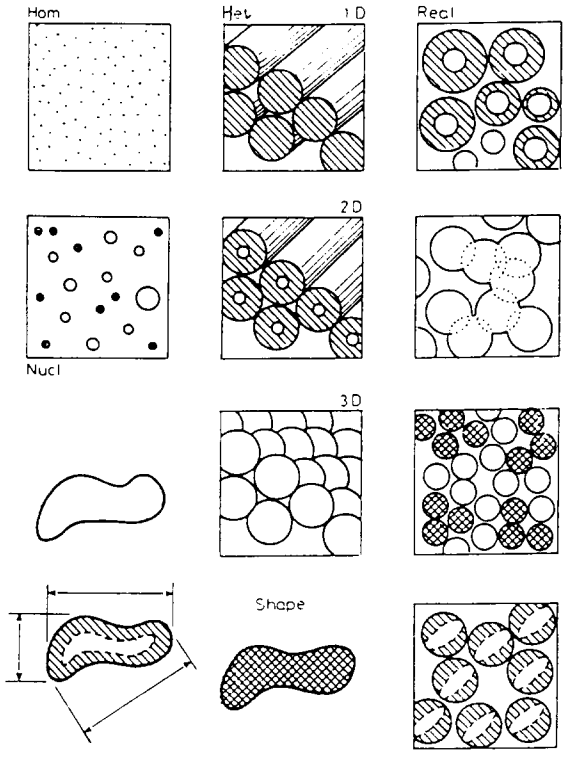

Fig. 1. Schematic diagram of a hypothetical transfer of the system geometry from a non-dimensional homogeneous-like model (obeying reaction order model $f(\alpha)=(1-\alpha)^n$, upper left) to the idealized heterogeneous model by introduction od dimensionality, due to the interface formation (nucleation obeying the logarithmic model $f(\alpha)=(1-\alpha)[\ln(1-\alpha)]^m$, lower left) and interface growth (controlled by either the linear law of a chemical reaction or parabolic law of diffusion, second column, compare table 1, R and D models). It is important to recall that the character of the kinetic description changes drastically from the concentration-dependent (HOM) to that of the interface-to-volume dependent (HET). The last column illustrates the behavior of real particles which does require to account for polydispersity, shielding and overlapping, unequal mixing and/or non-regular shapes and anisotropy (third column from top). Its kinetic modeling is mathematically difficult and can be formally accomplished by the introduction of an accomodation function, $h(\alpha)$, to multiply the basic monomolecular law $(1-\alpha)$, i.e. $f(\alpha)=(1-\alpha)h(\alpha)$, where $h(\alpha)$ can take the form of either function, $(1-\alpha)^{1-n}$, $[-\ln(1-\alpha)]^m$ and/or α^p. It helps particularly to fit the prolonged reaction tails due to the actual behavior of real particles and can match the particle non-sphericity in the view of morphology description in terms of characteristic dimensions (usually the longest particle length), interface (average boundary line) and volume (mean section area), see bottom left. For the sake of illustration, the original and reacted parts are distinguished by hatching.

essary. Therefore after eliminating the third exponential term in eq. (2) the final form obtained is

$$f(\alpha)=\alpha^m(1-\alpha)^n . \tag{3}$$

In the literature the equation (3) is cited as the Šesták–Berggren (SB) kinetic model. The exponents m and n have the significance of the kinetic parameters of the process. If the exponent m is set equal to zero, the remaining exponent n is then called the reaction order (RO). This approach is often used for a general description of all heterogeneous processes, although it has only limited applicability [6].

Both the SB and RO models can also be understood in terms of the accomodation function introduced by Šesták [7]. In this case the heterogeneous kinetics is assumed as a distorted case of the simpler homogeneous kinetics. The accomodation function then expresses the deviation of the more complex reaction mechanism from the ideal case; see fig. 1.

Recently we have shown [8] that the SB model cannot be considered as a general expression of the kinetic models (table 1) for the true (or fixed value) activation energy, E. Nevertheless, this is not so evident for any arbitrarily chosen value of the activation energy which is called here the apparent activation energy, E_{app} [2]. The validity of these procedures and the resulting functions when deriving the kinetic models in question was approved also for non-isothermal conditions elsewhere [9,10].

3.1. The reaction order model

Criado et al. [11] have shown that any TA curve can be described by the RO model instead of the true one for a certain value of the apparent activation energy. Recently it was found [12] that the ratio of the apparent and true activation energies (E_{app}/E) can be expressed for the apparent RO model by the following equation:

$$\frac{E_{app}}{E}=-\frac{f(\alpha_p)}{f'(\alpha_p)}\frac{n_{app}}{1-\alpha_p}, \tag{4}$$

where α_p is the degree of conversion at the maximum of the TA peak and n_{app} is an apparent kinetic exponent of the RO model. The value of n_{app} is characteristic for the true kinetic model but α_p depends also on the x_p (reduced activation energy at the maximum of the TA peak). Therefore the value of $E_{app}/$

E increases slightly with increasing x_p for diffusion models (i.e. D_2, D_3 and D_4). On the other hand, the ratio E_{app}/E decreases with increasing x_p for the A_n model as corresponds to the following equation [13]:

$$\frac{E_{app}}{E} = \frac{n-1}{x_p \pi(x_p)} + 1 , \qquad (5)$$

where n is the true kinetic exponent of the A_n model and $\pi(x)$ is the approximation of the temperature integral in the form [14]

$$\pi(x) = \frac{x^3+18x^2+88x+96}{x^4+20x^3+120x^2+240x+120} . \qquad (6)$$

It is noteworthy that the empirical relationship $E_{app}/E = 1.05\ E - 0.05$ found by Criado et al. [11] corresponds to the general equation (5) for $x_p = 38.3$.

The limiting values of the parameters n_{app} and E_{app}/E are summarized in table 2 for the kinetic models discussed.

3.2. The Šesták–Berggren model

The ratio of the apparent and true activation energies can be expressed for the SB model in the following form [12]:

$$\frac{E_{app}}{E} = -\frac{f(\alpha_p)}{f'(\alpha_p)}\left(\frac{n_{app}}{1-\alpha_p} - \frac{m_{app}}{\alpha_p}\right) . \qquad (7)$$

By rewriting eq. (1) for an apparent activation energy we obtain:

$$y_{app}(\alpha) = (d\alpha/dt)\exp(E_{app}/RT) . \qquad (8)$$

The function $y_{app}(\alpha)$ defined by eq. (8) is proportional to function $f(\alpha)$ that represents the apparent kinetic model of the process. Therefore, by plotting the $y_{app}(\alpha)$ dependence, the apparent kinetic model can be determined.

The function $y_{app}(\alpha)$ has a maximum at α_M for the SB model. It can be shown [#1] that the maximum is confined to the interval $0 < \alpha_M < \alpha_p$ and it can be used to determine the apparent kinetic exponent ratio [13]

$$\frac{m_{app}}{n_{app}} = \frac{\alpha_M}{1-\alpha_M} . \qquad (9)$$

It should be stressed that any change of the value of the apparent activation energy leads to a different value of the ratio m_{app}/n_{app}. Therefore both apparent kinetic exponents are mutually interdependent. A characteristics n_{app} versus m_{app} dependence can be found for each true kinetic model. These plots (full lines) calculated using eqs. (7) and (9) are shown in fig. 2. The dashed lines correspond to the different values of the maxima of the function $y_{app}(\alpha)$. An important feature of the n_{app}–m_{app} plot is that it is characteristic for the true kinetic model. Nevertheless, it can be seen that these plots are identical for the D_3 and R_3 models. There is also one common curve corresponding to the A_n model regardless of the values of the true kinetic exponent, n. Similar behavior was observed also for other types of reference plots [15,16]; see fig. 2.

Many works are concerned with the kinetic analysis of a single TA curve. However, these methods are somewhat problematic because of the apparent kinetic models. For example, the popular Freeman

Table 2
The values of apparent parameters ($x_p \to \infty$) for the RO model.

True model	n_{app}	E_{app}/E
A_n	1	n
D_2	0.269	0.483
D_3	0.666	0.5
D_4	0.420	0.495

[#1] It is evident that if the kinetic exponent, m, is equal to zero (i.e. for the RO model), then $\alpha_M = 0$. On the other hand E_{app} should not be negative. Therefore it follows from eq. (7) that α_M has to be lower than α_p.

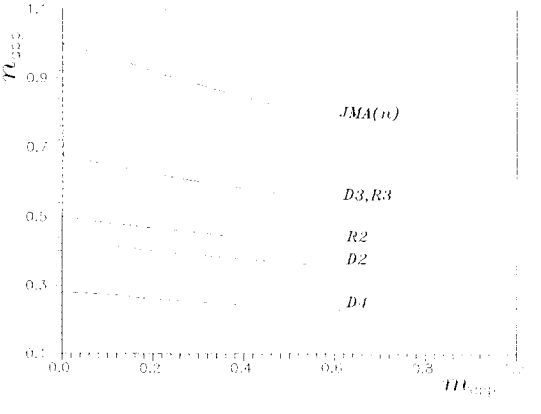

Fig. 2. Apparent kinetic exponents of the SB(m_{app}, n_{app}) corresponding to the D_2, D_3, D_4, R_2, R_3 and JMA(n) kinetic models.

and Carroll method [17] was derived for the RO model. Therefore, this method always gives apparent parameters n_{app} and E_{app} corresponding to the RO model regardless of the true kinetic model. Similarly, it must be borne in mind that the non-linear or multiple linear regression methods can lead to incorrect results because any TA curve can be interpreted within the scope of several apparent kinetic models (RO or SB) depending on the value of the apparent activation energy.

On the other hand, if the true activation energy is known, the SB kinetic model can be found very useful in real heterogeneous systems [6,18,19], where other kinetic models cannot be successfully used for a quantitative description of the experimental data.

4. Correlation of the kinetic parameters

Both the activation energy and the pre-exponential factor in eq. (1) are mutually correlated [20]. This correlation can be expressed by the following equation (see Appendix):

$$\ln A = a + bE , \qquad (10)$$

where a and b are constants. Any change in the activation energy is, therefore, "compensated" by the change of $\ln A$ as expressed by eq. (10). From this point of view, it seems that the methods of kinetic analysis aiming to ascertain all kinetic parameters from only one experimental TA curve are somewhat problematic. Similarly, as in the preceeding Section, we have to realize that this problem cannot be solved even using the most sophisticated non-linear regression algorithms unless the kinetic models or at least one kinetic parameter is a priori known.

The value of E can further consist of the elementary parts arising from the partial reaction steps [21], i.e. nucleation, interface chemical reaction and difussion, which became particularly important in the analysis of glass crystallization [22,23].

5. The kinetic analysis

The correlation of kinetic parameters and the apparent kinetic models does not allow us to perform correctly the kinetic analysis using only one experimental TA curve. This problem can be solved, however, if the true activation energy is known. Then the most probable kinetic model can be determined and subsequently the pre-exponential term is calculated. The method of kinetic analysis is described in the following sections.

5.1. Calculations of the activation energy

The calculation of the activation energy is based on multiple scan methods where several measurements at different heating rates are needed. Probably the most popular in this family is the Kissinger method [25] based on the equation derived from the condition for the maximum rate on a TA curve. A very similar method of calculation of activation energy is the Ozawa method [26].

An alternative method of calculation of the activation energy is the Isoconversional method which follows from the logarithmized form of the kinetic equation (1):

$$\ln(\mathrm{d}\alpha/\mathrm{d}t) = \ln\{Af(\alpha)\} - E/RT . \qquad (11)$$

The slope of $\ln(\mathrm{d}\alpha/\mathrm{d}t)$ versus $1/T$ for the same value of α gives the value of the activation energy. This procedure can be repeated for various values of α. So it easily allows one to check the invariance of E with respect to α, which is one of the basic assumptions in kinetic analysis. Hence, the isoconversional method can be recommended for the calculation of the E.

On the other hand, we cannot recommend the Freeman–Carroll method [17] because it was derived for the RO(n) model and, therefore, due to the mutual correlation of kinetic parameters, this method always gives apparent kinetic parameters n_{app} and E_{app} corresponding to the RO(n_{app}), regardless of the true kinetic model.

5.2. Determination of the kinetic model

Once the activation energy has been determined it is possible to find the kinetic model which best describes the measured set of TA data. It can be shown that for this purpose it is useful to define two special functions $y(\alpha)$ and $z(\alpha)$ which can easily be obtained by simple transformation of the experimental

data. These functions can be formulated as follows [27,28]:

$$y(\alpha) = (\mathrm{d}\alpha/\mathrm{d}t)\mathrm{e}^{x}, \tag{12}$$

$$z(\alpha) = \pi(x)(\mathrm{d}\alpha/\mathrm{d}t)T/\beta. \tag{13}$$

The function $y(\alpha)$ is proportional to the function $f(\alpha)$. Thus by plotting the $y(\alpha)$ dependence, normalized within the interval $\langle 0, 1 \rangle$, the shape of the function $f(\alpha)$ is obtained. The function $y(\alpha)$ is, therefore, characteristic for a given kinetic model, as shown in fig. 3, and it can be used as a diagnostic tool for kinetic model determination. The mathematical properties of the $y(\alpha)$ function for basic kinetic models are summarized in table 3. The function $y(\alpha)$ has a maximum $\alpha_M \in (0, \alpha_p)$ both for the HMA($n > 1$) and SB(m, n) model (see Appendix eqs. (A.13) and (A.14)).

It should be stressed that the shape of function $y(\alpha)$ is strongly affected by E. Hence the true activation energy is decisive for a reliable determination of the kinetic model because of the correlation of kinetic parameters.

Similarly we can discuss the mathematical properties of the function $z(\alpha)$. It is fairly easy to demonstrate (see Appendix, eq. A.10)) that the function $z(\alpha)$ has a maximum at α_p^∞ for all kinetic models summarized in tables 1 and 2. This parameter has characteristic values [13] for basic kinetic models as summarized in table 4. It is interesting that the α_p^∞ practically does not depend on the value of the activation energy used to calculate the function $z(\alpha)$ (in fact it varies within 1% of the theoretical value). An important fact is that α_p^∞ is invariant with respect to the kinetic exponent for the JMA(n) model. On the other hand, for both the RO(n) and SB(m, n) models, the parameter α_p^∞ depends on the values of the kinetic exponents as shown in fig. 4.

It is evident that the shape of the function $y(\alpha)$ as well as the maximum, α_p^∞, of the function $z(\alpha)$ can be used to guide the choice of a kinetic model. Both parameters α_M and α_p^∞ are especially useful in this respect. Their combination allows the determination of the most suitable kinetic model, as shown by the scheme in fig. 5. As we can see, the empirical SB(m, n) model gives the best description of TA data if $\alpha_p^\infty \not\equiv 0.632$ and $\alpha_M \in (0, \alpha_p)$. According to our experience, these conditions are fulfilled for some solid-state processes [29,30].

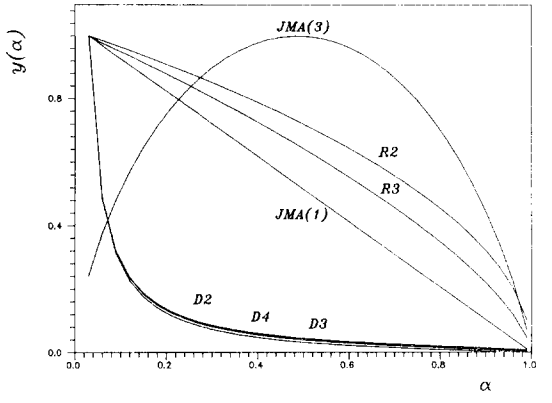

Fig. 3. Typical shapes of function $y(\alpha)$ for several kinetic models.

Table 3
Properties of the function $y(\alpha)$ for basic kinetic models

Model	$y(\alpha)$
JMA(n)	concave, for $n < 1$ linear, for $n = 1$ maximum, for $n > 1$
R2	convex
R3	convex
D2	concave
D3	concave
D4	concave

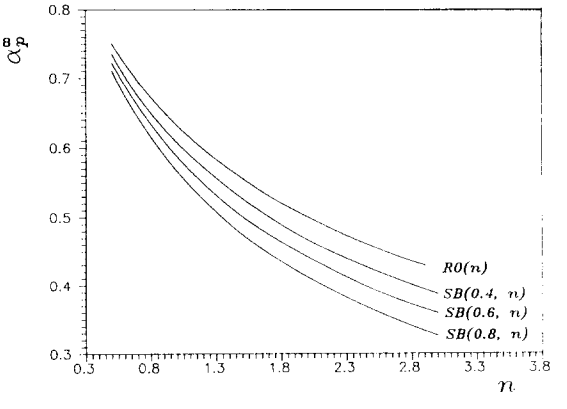

Fig. 4. The dependence of the maximum of the function $z(\alpha)$, α_p^∞, on the kinetic exponent, n, for the RO(n) and SB(m, n) kinetic models.

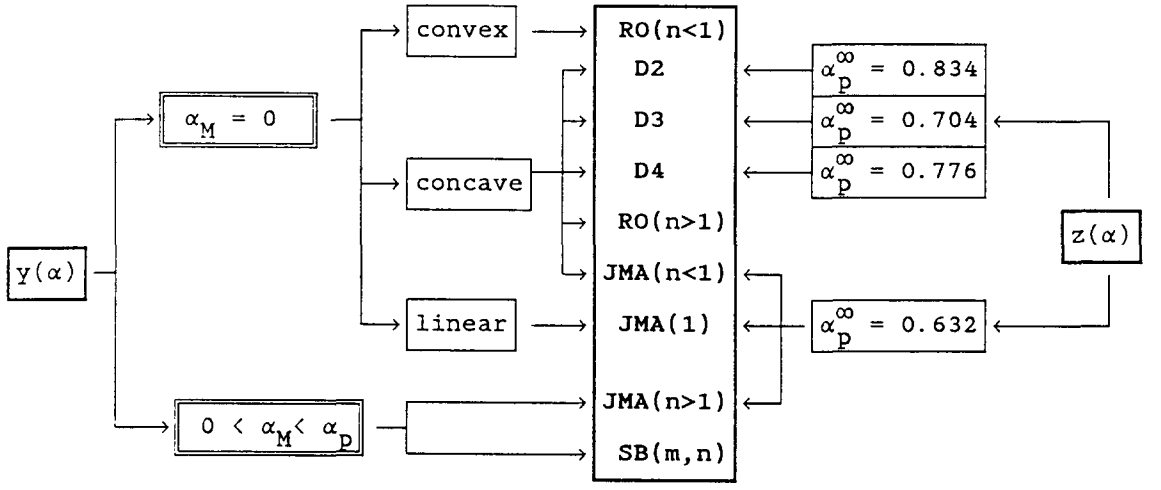

Fig. 5. Schematic diagram of the kinetic model determination.

5.3. Calculation of kinetic exponents

Once the kinetic model has been determined, the kinetic exponents n (or m) can be calculated for the RO(n), JMA(n) or SB(m, n) model. The calculation method depends on the kinetic model and is described below.

5.3.1. RO(n) model

The kinetic exponent $n \neq 0$ for this model can be calculated iteratively using the equation:

$$\alpha_p = 1 - \left(1 + \frac{1-n}{n} x_p \pi(x_p)\right)^{1/(n-1)} . \qquad (14)$$

This equation is obtained from eq. (A.4). We point out that it was derived originally by Gorbachev [5] for a simplified approximation: $\pi(x_p) = 1/(x_p + 2)$.

5.3.2. JMA(n) model

If the function y/α has a maximum at $\alpha_M \in (0, \alpha_p)$, i.e. for $n > 1$, then the kinetic exponent, n, is calculated using eq. (A.13) rewritten in a somewhat different form:

$$n = \frac{1}{1 + \ln(1-\alpha_M)} . \qquad (15)$$

If the function $y(\alpha)$ decreases steadily (i.e. $n \leqslant 1$), then the parameter, n, can be calculated by the Šatava method [31]

$$\ln[-\ln(1-\alpha)] = \text{const} - nE/RT , \qquad (16)$$

i.e. from the slope of the plot of $\ln(-\ln(1-\alpha))$ versus $1/T$. An alternative method of calculation is based on the following equation (obtained from eq. (A.4)):

$$n = \frac{1 - x_p \pi(x_p)}{\ln(1-\alpha_p) + 1} . \qquad (17)$$

It is known that the Šatava method [31] gives slightly higher values of the parameter n. On the other hand, eq. (1) gives lower ones. From our experience it seems that an average of these two values is a good approximation of the kinetic exponent.

5.3.3. SB(m, n) model

The kinetic parameter ratio, $p = m/n$, is calculated using eq. (A.14) rewritten as follows:

$$p = \alpha_M / (1 - \alpha_M) . \qquad (18)$$

Eq. (1) can be rewritten in the form:

$$\ln[(\mathrm{d}\alpha/\mathrm{d}t)\mathrm{e}^x] + \ln A + n \ln[\alpha^p (1-\alpha)] . \qquad (19)$$

The kinetic parameter, n, corresponds to the slope of linear dependence $\ln[(\mathrm{d}\alpha/\mathrm{d}t)\mathrm{e}^x]$ versus $\ln[\alpha^p(1-\alpha)]$ for $\alpha \in (0.2, 0.8)$. Then the second kinetic exponent is $m = pn$.

5.4. Calculation of the pre-exponential factor

Knowing the value of the activation energy and the kinetic model, the pre-exponential factor is calculated using the following equation [28]:

$$A = -\frac{\beta x_p}{Tf'(\alpha_p)} \exp(x_p) . \qquad (20)$$

6. Software for kinetic analysis

It is rather surprising that the mutual correlation of kinetic parameters as well as the apparent kinetic models are very often ignored even in the commercially available kinetic software. This is why a new software package TA-system was developed, based on the method of kinetic analysis of TA data described above.

The TA-system runs under MS DOS operating system on any IBM or compatible computer with at least 512 kB RAM and EGA or VGA graphics card. The system is very simple to use and it features flexible and interactive graphics capabilities which will present the results in an optimal way required by the user. Both data and graphs can be exported into most graphical and spreadsheet software packages.

The software package includes programs to calculate the activation energy from several sets of kinetic data at various heating rates. This value of activation energy is used by another program to calculate both $y(\alpha)$ and $z(\alpha)$ functions. The shape of these functions enables the proposal of the most probable kinetic model. Then the pre-exponential factors and kinetic exponents are calculated. This procedure is repeated for all heating rates. Therefore, we obtain several sets of kinetic parameters corresponding to various heating rates. If the mechanism of the process does not change during the TA experiment it would seem reasonable to expect that it will be possible to find the same kinetic parameters for different heating rates. The consistency of the kinetic model determined can also be assessed by comparing both experimental and calculated TA curves. Estimated kinetic parameters allow the calculation of isothermal α–t diagrams in order to predict the behaviour of the studied system under isothermal conditions.

7. Conclusions

It was shown that both activation energy and pre-exponential factor are mutually correlated. As a consequence of this correlation any TA curve can be described by an apparent kinetic model instead of the appropriate one for a certain value of apparent activation energy. Therefore, the kinetic analysis of TA data cannot be successful unless the true value of the activation energy is known.

Taking into account these facts, a new method of kinetic analysis of TA data has been proposed. This method allows the determination of the most suitable kinetic model and calculation of the meaningful kinetic parameters of the general kinetic equation.

It is possible to draw benefit in TA kinetics from its easiness and rapidity, provided that relatively low gradients are kept in the sample, which evidently requires as small a charge as possible. In the case that the sample must be larger, and if the reaction produces gaseous products, the technique of controlled rate thermal analysis (CRTA) [23] can provide more reliable results.

Appendix. The integral kinetic equation

If the temperature rises at a constant rate, β, then we obtain after integration of eq. (1) the equation:

$$g(\alpha) = \int_0^\alpha \frac{d\alpha}{f(\alpha)} = \frac{AE}{\beta R} e^{-x} \frac{\pi(x)}{x} , \qquad (A.1)$$

where $\pi(x)$ is an approximation of the temperature integral [3]. There are many approximate expressions of the $\pi(x)$ function in the literature. According to our experience the rational expression of Senum and Yang [14] is sufficient:

$$\pi(x) = \frac{x^3 + 18x^2 + 88x + 96}{x^4 + 20x^3 + 120x^2 + 240x + 120} . \qquad (A.2)$$

A.1. The condition for the maximum of the TA curve

Differentiating eq. (1) with respect to time, the following equation is obtained [19]:

$$d^2\alpha/dt^2 = [\beta/T\pi(x)]^2 f(\alpha)g(\alpha)[f'(\alpha)g(\alpha) + x\pi(x)] . \quad (A.3)$$

The condition for the maximum of the TA curve is obtained by setting eq. (A.3) equal to zero:

$$-f'(\alpha_p)g(\alpha_p) = x_p\pi(x_p) . \quad (A.4)$$

A.2. Correlation of kinetic parameters

Substitution of eq. (A.1) into eq. (A.4) gives eq. (A.5):

$$-f'(\alpha_p)Ae^{-x_p} = \beta R x_p^2/E . \quad (A.5)$$

Eq. (A.5) can be rewritten after converting it to logarithms in the following form:

$$\ln A = a + bE , \quad (A.6)$$

where $b = 1/RT_p$ and $a = \ln[-\beta x_p/Tf'(\alpha_p)]$.

A.3. The maximum of the z(α) function

An alternative expression for the reaction rate is obtained by combining eqs. (1) and (A.1):

$$d\alpha/dt = [\beta/T\pi(x)]f(\alpha)g(\alpha) . \quad (A.7)$$

After a rearrangement of eq. (A.7) the following equation can be written for $z(\alpha)$:

$$z(\alpha) = \pi(x)(d\alpha/dt)T/\beta = f(\alpha)g(\alpha) . \quad (A.8)$$

Differentiating eq. (A.8) with respect to α we obtain eq. (A.9):

$$z'(\alpha) = f'(\alpha)g(\alpha) + 1 . \quad (A.9)$$

By setting eq. (A.9) equal to zero, we get the equation (A.10) that must be fulfilled by α_p^∞ at the maximum of $z(\alpha)$:

$$-f'(\alpha_p^\infty)g(\alpha_p^\infty) = 1 . \quad (A.10)$$

An identical result is obtained from eq. (A.4) when x_p is infinite because in this case

$$\lim_{x_p \to \infty} [x_p\pi(x_p)] = 1 . \quad (A.11)$$

Hence the value of α_p^∞ also corresponds to the maximum of a hypothetical DSC or DTA peak for $x_p \to \infty$.

A.4. The maximum of the y(α) function

Comparing eqs. (1) and (6), the function $y(\alpha)$ can be expressed as follows:

$$y(\alpha) = Af(\alpha) . \quad (A.12)$$

Therefore, the condition for the maximum of the function $y(\alpha)$ can be written as $f'(\alpha) = 0$. Analyzing this condition we can find that the *D*2, *D*3, *D*4 and RO(n) kinetic models have a maximum at $\alpha_M = 0$. It can also be shown that there is a maximum of the function $y(\alpha)$ at $0 < \alpha_M < \alpha_p$ for both the JMA(n) and SB(m, n) models that depends on the value of the kinetic exponents. The condition for a maximum of the JMA($n > 1$) model is given by equation:

$$\alpha_M = 1 - \exp[(1 - n/n)] . \quad (A.13)$$

Similarly, the condition for a maximum of the SB(m, n) model is expressed as follows:

$$\alpha_M = m/(m+n) . \quad (A.14)$$

References

[1] J. Šesták, ed., in: Reaction kinetics by Thermal Analysis, Special issue of Thermochim. Acta 203 (1992).
[2] J. Šesták, J. Thermal Anal. 16 (1979) 503; 33 (1988) 1263.
[3] J. Šesták, Thermophysical Properties of Solids, Their Measurements and Theoretical Thermal Analysis (Elsevier, Amsterdam, 1984).
[4] J. Šesták and G. Berggren, Thermochim. Acta 3 (1971) 1.
[5] V.M. Gorbatchev, J. Thermal Anal. 18 (1980) 194.
[6] J. Málek and V. Smrčka, Thermochim. Acta 186 (1991) 153.
[7] J. Šesták, J. Thermal Anal. 36 (1990) 1977.
[8] J. Málek and J.M. Criado, Thermochim. Acta 175 (1991) 305.
[9] J. Šesták, in: Thermal Analysis, Proc. 2nd ESTAC, Aberdeen, ed. D. Dollimore (Wiley, London, 1981) p. 115.
[10] T. Kemény and J. Šesták, Thermochim. Acta 110 (1987) 113.
[11] J.M. Criado, D. Dollimore and G.R. Heal, Thermochim. Acta 54 (1982) 159.
[12] N. Koga, J. Šesták and J. Málek, Thermochim. Acta 188 (1991) 333.
[13] J. Málek, Thermochim. Acta 200 (1992) 257.

[14] G.I. Senum and R.T. Yang, J. Thermal Anal. 11 (1977) 445.
[15] J.M. Criado, J. Málek and A. Ortega, Thermochim. Acta 147 (1989) 377.
[16] J. Málek and J.M. Criado, Thermochim. Acta 164 (1990) 199.
[17] E.S. Freeman and B. Carroll, J. Phys. Chem. 62 (1958) 394.
[18] L. Tichý and P. Nagels, Phys. Status Solidi A87 (1988) 769.
[19] J. Málek, J. Non-Cryst. Solids 107 (1989) 323.
[20] N. Koga and J. Šesták, Thermochim. Acta 182 (1991) 201.
[21] J. Šesták, Phys. Chem. Glasses 15 (1974) 137.
[22] J. Šesták, Thermochim. Acta 98 (1986) 339.
[23] N. Koga and J. Šesták, J. Thermal Anal. 37 (1991) 1103.
[24] J. Málek, J.M. Criado, J. Šesták and J. Militký, Thermochim. Acta 153 (1989) 429.
[25] H.E. Kissinger, Anal. Chem. 29 (1957) 1702.
[26] T. Ozawa, J. Thermal Anal. 2 (1979) 301.
[27] J.M. Criado, J. Malek and A. Ortega, Thermochim. Acta 147 (1989) 377.
[28] J. Málek, Thermochim. Acta 138 (1989) 337.
[29] J. Málek and V. Smrčka, Thermochim. Acta 186 (1991) 153.
[30] J. Málek, J. Non-Cryst. Solids 107 (1989) 323.
[31] V. Šatava, Thermochim. Acta 2 (1971) 423.
[32] J. Málek, J.Šesták, F. Rouquerol, J. Rouquerol, J.M. Criado and A. Ortega, J. Thermal Anal. 38 (1992) 71.